



Structural changes in sheep tibia bone undergoing biomaterial scaffold implant

Craig Maxwell



**Faculty of Industrial Engineering,
Mechanical Engineering and Computer Science
University of Iceland
2012**

Structural changes in sheep tibia bone undergoing biomaterial scaffold implant

By Craig Maxwell

60 ECTS thesis submitted in partial fulfillment of a
Magister Scientiarum degree in Mechanical Engineering

Advisor(s)

Sigurður Brynjólfsson

Paolo Gargiulo

Faculty Representative

Olafur Petur Palsson

Faculty of Industrial Engineering, Mechanical Engineering
and Computer Science
School of Engineering and Natural Sciences
University of Iceland
Reykjavik, 2012

60 ECTS thesis submitted in partial fulfillment of a *Magister Scientiarum* degree in
Mechanical Engineering

Copyright © 2012 Craig Maxwell
All rights reserved

Faculty of Industrial Engineering, Mechanical Engineering and Computer Science
School of Engineering and Natural Sciences
University of Iceland
VR-II, Hjarðarhaga 2-6,
IS-107 Reykjavik,
Iceland.

Telephone: +354 525 4648

Abstract

Bone fracture is a common occurrence with most people having, or knowing someone who has experienced it. This thesis displays quantitative results on the growth and strength of new material formed in a fracture gap by analysing the density and volume of the implanted biomaterial scaffold and the new material formed alongside gait and Finite Element Analysis (FEA) of external factors which can have an effect on the remodeling process. The main goal of this thesis is to present methods to provide quantitative results specifically related to the formation of new material with the implant of a biomaterial scaffold.

Skeletally mature sheep were used in the trial in which 21 sheep were randomized into 3 groups of 7. Each group had a 25 mm induced fracture in the rear right leg tibia of each sheep into which three scaffold groups were placed. CT scans were taken of the tibia and quantitative results were gathered on several aspects of the scaffold, new growth material and also of external stimulation factors. External stimulation factors measured were the gait of the sheep, the screw forces experienced and stress shielding due to the fracture plate.

All groups displayed new material growth to some extent with some specimens displaying healing patterns similar to those expected in secondary healing. It was shown that the sheep were using the injured legs but not to the extent of first thought which coupled with the stress shielding found in the plate can be expected to affect the remodeling process.

Útdráttur

Þetta verkefni fjallar um áhrif lífvirkar burðargrindar á beinvöxt og styrk beins sem myndast eftir beinbrot. Einnig er framkvæmd göngugreining og gert element líkan af beini og spengingu til að athuga áhrif ytri þátta á beinvöxt. Þéttleiki nýja beinsins og rúmmál við burðargrindina var ákvarðað.

Markmiðið var að þróa aðferð til að mæla nýmyndun beins og áhrif lífvirkar burðargrindar. Í þessu verkefni voru notaðar 21 fullþroska kind. Var þeim skipt í 3 hópa. Tekin var 25 mm bútur úr hægri sköflungi á hverri kind og mismunandi lífvirkar burðargrindur sett í hvern hóp. Fylgst var með kindunum í nokkra mánuði. Að lokum var tekin tölvusneiðmynd af beinbrotinu og beinvöxtur, þéttni og áhrif spelkunnar ákvarðað. Ytri þættir sem hafa áhrif á beinvöxt eru m.a. álag á fót og var álagið metið með göngugreiningu, einnig spennan sem myndast við spengingu og skrufugöt.

Beinið óx í öllum þremur hópum og í nokkrum sýnum var beinvöxtur umtalsverður. Sýnt var fram á að kindurnar notuð veika fótinn, en ekki í þeim mæli sem í fyrstu var talið. Það, ásamt spennunni sem spengingin olli hefur áhrif á beinvöxtinn.

*Dedicated to all the sheep
involved in the trial.*

Table of Contents

1. Introduction	1
1.1. Motivation	1
1.2. Project Aim	1
1.3. GENIS Project collaboration.....	1
1.4. Chapter Contents	1
2. Bone Biology, Properties, Fractures and Fracture Fixation.....	3
2.1. Introduction	3
2.2. The Musculoskeletal System.....	3
2.2.1. Anatomical Overview	3
2.2.2. The Functions of the Musculoskeletal System.....	4
2.2.3. Immobilization or Disuse of Limbs and the Effect on Bone.....	5
2.2.4. Bone Remodelling in Bone Fractures	6
2.3. Factors Affecting Bone Strength.....	7
2.3.1. Material Properties	7
2.3.2. Bone Mass and Remodelling.....	8
2.4. Internal Fracture Fixation Methods.....	8
2.4.1. Screws	8
2.4.2. Fracture Plates	9
2.4.3. Static and Dynamic Fixation	9
3. Material and Methods.....	11
3.1. Introduction	11
3.2. Clinical Scaffold Technology.....	11
3.3. Clinical Trial Procedure	12
3.4. Gait	14
3.5. Spiral Computed Tomography	15
3.6. Medical Image Processing	16
3.6.1. Importing Data	16
3.6.2. Segmentation and Modelling	17
3.6.3. Morphological Changes	19
3.6.4. Absolute Screw Movement	20
3.6.5. Proximal and Distal Density Loss	20
3.7. Finite Element Modelling.....	21

3.7.1. Finite Element Method.....	21
3.7.2. Post-Operative Model	22
3.7.3. Meshing in 3-Matic	23
3.7.4. Material Assignment	23
3.7.5. Contact Regions	24
3.7.6. Application of Forces and Fixtures	25
3.8. Protocols and Calibration	25
4. Results.....	27
4.1. Introduction	27
4.2. Gait	27
4.2.1. Stride length	27
4.2.2. Mean Stance Time.....	28
4.2.3. Peak Pressure Index	29
4.3. Morphological Changes in Bone and Scaffold	31
4.3.1. Scaffold Volume	31
4.3.2. Scaffold Mean Density.....	32
4.3.3. Scaffold mean Density and Volume Correlation	33
4.3.4. Scaffold Density Distribution.....	34
4.3.5. Scaffold Density Distribution Slices	35
4.3.6. New Material Volume	36
4.3.7. New Material Mean Density	37
4.3.8. New Material Density and Volume Correlation	38
4.3.9. New Material Density Distribution	39
4.3.10. New Material Density Distribution Slices	40
4.3.11. Absolute Screw Movement	42
4.3.12. New Material volume, density and screw movement correlation	43
4.3.13. Proximal and Distal Density Loss	44
4.4. Finite Element Analysis	45
4.4.1. Screw reactions	45
4.4.2. Stress Shielding	46
5. Discussion	47
6. Conclusions	49
References	51

List of Tables

Table 4.1. Density regions for Scaffold Segmentation	36
Table 4.2. Density Regions of new material.	41
Table 4.3. Density values (HU) of proximal and distal volumes showing pre and post-surgery procedures proximally and distally and also losses proximally and distally and percentage loss proximally and distally.....	44

List of Figures

Figure 2.1. Skeletal arrangement of a skeletally mature sheep [2].	3
Figure 2.2 Composition of Compact Bone and Cancellous Bone [7].	5
Figure 2.3. Secondary Fracture Healing- The Three phases of fracture healing with relative time duration are pictured. The initial soft callus is converted into hard callus and then mineralized into bone during the remodelling phase. [21].....	7
Figure 3.1. a, b, c. Operation procedure showing resection of bone (a), placement of fixture device and scaffold (b) and attachment of fixture device (c).	12
Figure 3.2. a, b, c. Removal Procedure showing removal of cast (a), insertion of formalin (b), removal of leg (c) and removed tibia with fracture plate (d)	13
Figure 3.3. GAITFour setup showing Mat and sensor pads (left hand side of mat)	14
Figure 3.4. Block diagram of a CT scanner [37].....	15
Figure 3.5. Calculation of CT or Hu number [39].	16
Figure 3.6. Scanning of Removed Tibia	16
Figure 3.7. (a) 2-D DICOM files obtained from CT scan, (b) Stacked DICOM files in the MIMICS program, (c) Resultant 3-D model created in MIMICS from the stacked DICOM files.....	17
Figure 3.8. Segmentation Process Showing Thresholding (A) and region growing (B) with segmentation selection Process shown in the middle.....	18
Figure 3.9. Edited mask for region of interest (left), 3D model constructed	19
Figure 3.10. Measurement of screw movement showing typical scan after 2 weeks (left)	20
Figure 3.11. (a) A general two-dimensional domain of field variable $\phi(x,y)$. (b) A three node finite element defined in the domain, (c) Additional Elements showing a partial finite element of the domain [41].	21
Figure 3.12. (Left) Post-operation setup, fracture plate assembly and tibia after induced fracture and plate application operation. (Right) Fracture plate and screw assembly which was imported into mimics.	22
Figure 3.13. (Left) Meshed model and (right) inspection tree with mesh information.....	23
Figure 3.14. (Left) Material Assignment of homogeneous bone densities and (Right) proximal and distal sections with 10 density regions both shown with fracture plate assembly.	24
Figure 3.15. Post-op model shown with highlighted contact regions between screw and bone.	24
Figure 3.16. (A) Forces Applied to Model Proximal, (B) Distal with (C) fixed support at centre screw holes.	25

Figure 4. 1. Both walks by all three sheep with the average stride length shown for all limbs during the walk.	27
Figure 4. 2. Average mean stance time shown for all specimen walks and for all limbs during the walks.	28
Figure 4. 3. Average Peak pressure index shown for all sheep walks for all limbs during the walks.	29
Figure 4. 4. Peak Pressure index per footfall for a complete walk of injured sheep C2.	30
Figure 4. 5. Scaffold Volumes from groups B and C and respective control scaffolds.	31
Figure 4. 6. Groups B and C scaffold mean density and control scaffolds and the average mean control density.	32
Figure 4. 7. . Correlation between scaffold types and controls showing mean density and volume for all groups.	33
Figure 4. 8. Density regions displayed as a percentage of total volume of scaffold, control and control bone specimens with the densities given in Hounsfield Units.	34
Figure 4. 9. a, b Two specimen slices (left to right a and b)	35
Figure 4. 10. a, b Two specimen slices (left to right a and b).	35
Figure 4. 11.a,b Control Scaffolds group B and C left and right respectively	35
Figure 4. 12. New material volume for all specimens from all groups and the average bone volume from the same removed section from the contralateral specimen.	36
Figure 4. 13. New Material mean density shown in all specimens from all groups with the average control mean density displayed with a dashed blue line.	37
Figure 4. 14. Volume and Mean density correlation in new material formations from the three specimen groups and removed bone section.	38
Figure 4. 15. New Material Density Ranges.	39
Figure 4. 16.a, b, c High cross section volume with low density distribution throughout.	40
Figure 4. 17.a, b, c Minimal gap closure and similar density distribution to control bone at fracture ends.	40
Figure 4. 18.a, b, c Minimal Gap closure and similar density distribution to control bone at fracture ends.	40
Figure 4. 19. Removed Control Bone Section.	40
Figure 4. 20. Absolute Movement of screws for the three groups.	42
Figure 4. 21. New material density, volume and absolute screw movement for each group.	43
Figure 4. 22. Density distribution in proximal and distal sections. Higher density materials are shown with darker colours.	44
Figure 4. 23.a, b Stresses on distal and proximal section of bone showing homogeneous density (left specimens) and applied CT density data (right specimens).	45
Figure 4. 24. Stresses shown on fixture plate with anatomically correct and identical cross section all with homogeneous density distribution.	46

Nomenclature

LISS – Less invasive stabilization system

CT – Computed tomography

FEA – Finite element analysis

RP – Rapid prototyping

HU – Hounsfield units

DICOM – Digital imaging and communications system

FEM – Finite element method

QUASAR – Quality assurance aystem for advanced radiotherapy.

Acknowledgements

I would most like to thank my family as without them and their support this would not have been possible. I would also like to thank my ‘new’ Icelandic family who have made me feel welcome and helped me whenever needed.

I would also like to thank my supervisors Paolo Gargiulo, who made me feel very welcome and provided me with countless hours of assistance and guidance through my studies, and Sigurður Brynjólfsson who also gave up hours of personal time to help with my studies and answer any questions I had. Without them I would never have been able to finish my studies.

I also owe a lot of thanks to all the students and staff at the science, education and innovation department of Landspítali and Reykjavík University for allowing me to use their equipment and providing a comfortable and enjoyable workspace during my studies, they made me feel part of the team and made my work environment both enjoyable and knowledge rich, and also made sure I had plenty of cake and coffee every day.

Finally I would like to thank the members of the ARM consortium, Jóhannes, Jón and the staff from genis for all their help during the project and for allowing me to be part of the trial as without them this thesis would never have been possible, and Halldor Jr and all the staff at Landspítali for all the knowledge they passed on and for countless hours they took out of their day to assist in the project and help me understand the tasks they were performing.

1. Introduction

1.1. Motivation

There are several conditions in which fractured bone may not be capable of healing itself such as a massive traumatic bone loss or bone resection in which the bone defect exceeds a critical size and will not heal correctly with the help of a mechanical fixture alone resulting in non-union of the fracture ends [1]. In cases like these a clinical scaffold is inserted into the bone gap to assist and promote bone formation. Biomaterial scaffolds provide a 3-D structure for the bone to form in and around to enable the bone to heal properly in fractures out with the critical length size.

1.2. Project Aim

The main aim of the study was to display techniques used to monitor and quantify tissue changes within sheep tibiae bone resections as a result of different scaffold implantations and their ability to promote and sustain new bone growth. The effectiveness of the new scaffold was quantified with the volume of new material created, the quality of the new material formed in terms of density, density distribution and with the comparison to the existing clinical scaffold technology results obtained during the trial. External factors investigated were gait, stress shielding and screw movement forces to analyse how these factors could possibly have affected the formation of new material.

1.3. GENIS Project collaboration

GENIS ehf. is a bio-medical development company who are currently working on a bone repair project supported by the Technology Development Fund. The project is an extremely successful collaborative effort between GENIS ehf., scientists at University of Iceland, the University Hospital and the innovation Centre Iceland together named the ARM-Consortium. The project involves development of a prototype of new bone void filler and an extensive program of biological testing in sheep models. The prototype filler has a unique composition comprising polymers specially optimized for biological performance and is being compared during this test in a sheep tibia model against one of the world market leaders.

1.4. Chapter Contents

This thesis is divided into four main chapters with chapter two focusing on background information on bone biology, properties of the bone, fractures of the bone and fracture fixation. The Purpose of chapter two is to provide some background information on subjects and concepts that will be discussed further in subsequent chapters.

Chapter three displays and discusses the materials and methods used during the trial. Here, clinical scaffold technology is discussed along with a brief description of the trial procedure and an introduction to the computational methods employed during the study.

Chapter four is the results section and displays the most important findings during the trial along with brief explanations of why the measurements were taken and what the results show.

Chapters five and six are the discussions and conclusions of the thesis. Here a summary is given on the results with explanations as to what the results illustrate and also conclusions on the thesis are also given.

2. Bone Biology, Properties, Fractures and Fracture Fixation

2.1. Introduction

Bone is a uniquely structured material which has been the subject of many studies by the engineering community, not only because of its unique structure which has the ability to remodel itself over time, but because this remodelling process takes place to alter the mechanical properties to satisfy the requirements of the bone in the body. The information in chapter one will provide a basic understanding of the bone material, the remodelling process and the skeletal structure along with factors that affect bone strength as well as fracture types and also fracture fixation methods, the information covered in chapter one will allow for the development of subsequent topics and concepts.

2.2. The Musculoskeletal System

2.2.1. Anatomical Overview

The sheep skeleton (figure 2.1) consists of many rigid organs called bones that move, support and protect the various organs of the body. There are five types of bone which are shaped to perform various tasks required of the body.

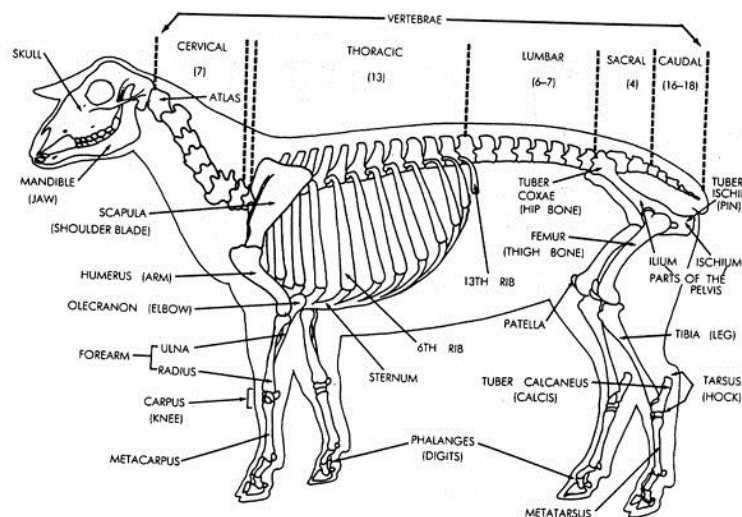


Figure 2.1. Skeletal arrangement of a skeletally mature sheep [2].

- Long bones - Characterized by a shaft (the diaphysis) which is much longer than it is wide. Most bones of the limbs are long bones.
- Short bones - Roughly cube shaped, the phalanges, found in the foot of the sheep, are short bones.
- Flat bones- Thin and generally curved. Most of the bones of the skull are flat bones.
- Irregular bones - Do not fit into the above categories and are irregular and complex in shape. The bones in the spine are irregular bones.
- Sesamoid bones – Bones that are embedded in tendons. The patella is an example of a sesamoid bone [3].

2.2.2. The Functions of the Musculoskeletal System

The musculoskeletal system has four main functions:

Haematopoiesis- Trabecular bone, which is a highly porous bone found mostly at the ends (epiphyses) of long bones, provide sites for the formation of red blood cells, a process known as haematopoiesis [4].

Mineral Storage- The bones of the body act as reserves of minerals important for the body [3]. The continuous process of the remodelling of bone (the resorption and formation of bone tissue) is one of the ways the minerals in the bloodstream are altered [4].

Protection of the Vital Organs- The internal organs of the body are protected by the various structures of the skeleton that allow it to absorb large amounts of energy yet remain lightweight [4].

Support and Motion- The primary function of the skeletal system is to provide force and motion for mobility during daily activity.

2.2.3. Composition of Bone

Cortical or compact bone (figure 2.2) is the densest bone in the skeleton [3] and is the hard outer layer of the bone. It is this tissue that gives bones their smooth, white, solid appearance. Trabecular or cancellous bone is composed of a network of rod and plate like elements allows room for blood vessels and marrow. The primary types of cell that constitute the bone are: osteoprogenitor cells, osteoblasts, osteocytes, osteoclasts and bone lining cells [5].

Osteoprogenitor cells – There are two types of osteoprogenitor cells, one producing bone-forming osteoblasts, and the other producing bone-resorption osteoclasts. Both types are commonly found near the bone surface [5].

Osteoblasts – Osteoblasts descend from osteoprogenitor cells and produce a protein mixture known as osteoid which mineralizes to become bone.

Osteocytes – Originate from osteoblasts that have become trapped by the bone matrix that they themselves produce. They have also been shown to act as mechano-sensory receptors – regulating the bones response to stress and mechanical load.

Osteoclasts – These are the cells responsible for bone resorption and are located on bone surfaces [3].

Bone Lining Cells – These cells cover most resting bone surfaces and serve as a barrier separating fluids filtering through the bone [6].

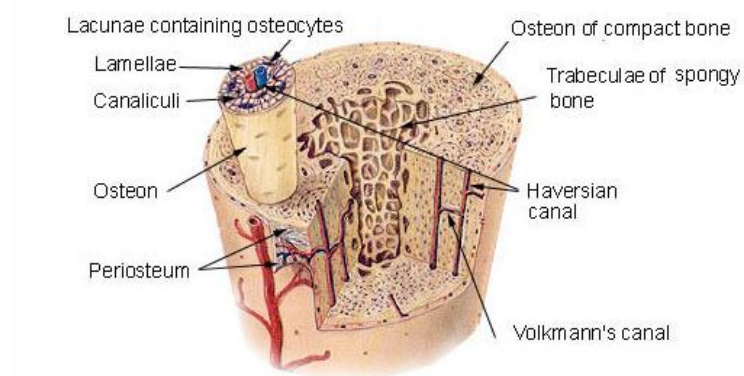


Figure 2.2 Composition of Compact Bone and Cancellous Bone [7].

2.2.4. Immobilization or Disuse of Limbs and the Effect on Bone

Immobilization of bone for extended periods of time has been shown to result in considerable amounts of bone resorption [8]. The duration of immobilization is a major determinant of the severity of bone loss as bone tissue has been shown to develop under the constant influence of stimulation such as the earth's gravity and locomotion [9]. Compared to static weight bearing ground reaction forces, dynamic loading generated by muscle contractions during locomotion is of paramount importance as the skeletal system adapts to different stimuli. Basic bone adaption can take place on trabecular and/or cortical surfaces irrespective of the cause of resorption, if mechanical stimulation decreases compared to normal levels, the unloaded bones loose mass and become structurally less rigid [10,11]. It is current understanding that the bone cells act a feedback system in which they sense the surrounding strain, and add or remove to bone to maintain the strain levels at a normal level, a removal of this strain would cause a constant removal of bone until the stress level was as before.

2.2.5. Bone Remodelling in Bone Fractures

Bone is a complex, dynamic tissue composed of both mineral and organic phases that constantly undergoes remodelling even once growth and modelling of the skeleton have been completed [12]. As the skeleton is the body's main load bearing structure, it is often damaged due to the extensive time it must function and the unusual loads to which it is often subjected [13]. Fluctuations in bone mass density can lead to fractures as the load bearing capacity of the bone alters as the bone mass density changes. Remodelling results in the resorption of bone where it is not needed (areas of low stress) and deposition of bone where it is needed (areas of high stress) [14]. When motion is minimized, but not eliminated across an existing fracture gap, healing must go through a fibrous callus repair phase that is converted to bone which is known as Secondary Healing [4].

Secondary healing often known as callus healing or indirect healing (figure 2.3), takes place in fractures treated by closed reduction or with semi-rigid fixation methods which allow the fractured bone to be approximated for axial alignment but not compression. Due to the fracture gap not being compressed and rigidly fixed, motion occurs at the gap site in secondary healing and the formation of callus is a normal reaction in this unstable healing environment. The difference between beneficial motion in the fracture gap which induces callus formation, and too much motion which leads to non-union, is extremely small [15].

The process of secondary healing is characterized by three discrete, yet overlapping stages of inflammation, repair, and remodelling [16]. The immediate inflammatory stage is triggered by various sources in which mesenchymal stem cells (cells which can change into various other cell types) are committed to become the cell types [17,18] required for the early formation of a soft callus which is eventually replaced by a hard callus during the repair phase [19]. Re-establishing sufficient blood supply is imperative to healing throughout all stages of fracture healing, but this is especially important during the repair stage in which the damaged cells are removed and the weak clotted haematoma is repaired (provided adequate stabilization of the fracture gap and appropriate loading) with a more substantial, bony or hard callus [20]. The 'collar of callus' that forms around a fracture provides provisional stability (through its mass) and strength (through its geometry) to ensure that healing may progress [3]. This is achieved when cells in the callus fail to multiply, enlarging and initiating calcification. Osteoclasts resorb the calcified cartilage and osteoblasts subsequently secrete osteoid. The osteoid is mineralized to form woven or primitive bone. Within the soft primitive callous, the bone and connective tissues are poorly organized and not aligned in a manner to resist excessive force and although the stiffness of the bone is more similar to mineralized tissue, the strength remains low [4]. The remodelling stage of fracture healing can last months to several years. The ultimate goal of the remodelling stage is to restore bone to its original strength [4] and follows the normal remodelling pattern of resorption and deposition of bone density.

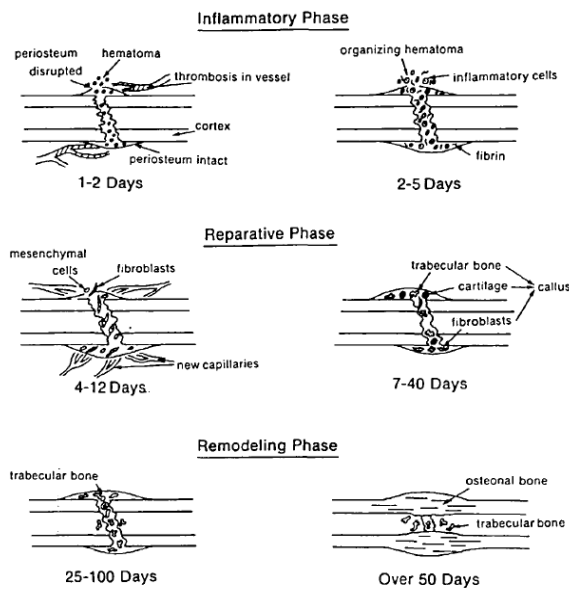


Figure 2.3. Secondary Fracture Healing- The Three phases of fracture healing with relative time duration are pictured. The initial soft callus is converted into hard callus and then mineralized into bone during the remodelling phase. [21].

2.3. Factors Affecting Bone Strength

2.3.1. Material Properties

The material properties of bone are determined by the properties of the elements that make up the structure of the bone and are independent of the bones size or shape [22]. The mineral phase of bone is responsible for both mechanical and stationary functions. Bones in the skeleton are not uniformly mineralised, but display a varying distribution of mineralisation at any given skeletal site. While an increased level of bone mineralisation is accompanied by an increase in the stiffness of the bone, it also exhibits reduced toughness (energy required to cause a fracture) of the bone [23]. This means that as the mineralisation at a specific skeletal site increases, the bone becomes more brittle and requires less energy to fracture [24].

2.3.2. Bone Mass and Remodelling

An important part of any structure is its mass and bone mass has a large role in the strength of bone [24]. During growth and modelling there is a substantial accumulation of bone mass which provides an increase of biomechanical strength as there is typically an expansion at the endocortical and the periosteal (inside and outside of the cortical bone) surfaces, leading to a wider diameter bone. However, during times of rapid bone accumulation, such as during growth, the mean degree of mineralisation is low [25]. During very rapid growth there have been reports of increased fracture susceptibility, perhaps as a result of increased cortical porosity [26], therefore, while there are rapid gains made in bone mass, there is still a component of weakness, perhaps as a consequence of some of the other components of bone quality degrading [24].

During growth, remodelling plays a small part in the changes in bone mass, but after skeletal maturation it plays a dominant role. Small losses in bone mass are observed over time in adults, which is thought to be a consequence of small imbalance between osteoclast and osteoblast activity. These losses, either gradual or rapid, decrease the mass of bone which will directly impact bone strength [24]. The remodelling process itself momentarily decreases the strength of the area that is undergoing remodelling as osteoclastic activity creates resorption pits which decrease both the local mass of bone and the architectural integrity of the site during mechanical loading [27].

2.4. Internal Fracture Fixation Methods

A broken bone must be fixed into the correct orientation and supported until it is strong enough to bear weight to enable the fracture to heal with proper union and alignment. Until the last century, physicians relied on casts and splints to support the bone from the outside the body (external fixation), but the development of sterile surgery reduced the risk of infection so that doctors could work directly with the bone and could implant materials in the body [28].

There are many different types of internal fixation devices that are used to achieve prompt and, if possible, full function of the injured limb with rapid rehabilitation of the patient. The majority of internal fixation implants are currently made of stainless steel, but occasionally, less strong but biologically superior and more elastic titanium implants are favoured.

2.4.1. Screws

Bone screws are a basic part of modern internal fixation [29,30]. They can be used independently or in combination with particular types of implants.

Locking screws are incorporated in more recent plate designs. In LISS (less invasive stabilization system, figure 2.4) the screws tighten to the plate; this locked screw-plate connection provides the

path for load transmission to the plate. Bio-mechanically, locking screws function more like a bolt than a screw and the system acts generally like an internal-external fixator [31] as the plate is not in direct contact with the bone as shown in figure 2.4 below.

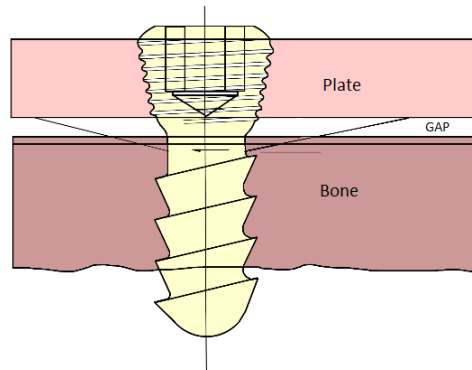


Figure 2.4. Gap between plate and bone limits the disruption of periosteal blood supply while providing support to the fractured bone.

2.4.2. Fracture Plates

Standard plate fixation requires exposure of the fracture site, haematoma evacuation and, if possible, reduction of the fracture. Bridge plating is used in comminuted unstable fractures (crushed segments of bone) or large fracture gaps where anatomic restoration and absolute stability cannot be achieved. In bridge plating the fracture plate is applied to the two main fragments and spans the length of the fracture. The plate is used to provide proper length, axial alignment and rotation but is limited for any applied load [31]. The LISS system is advanced towards the fracture site through a small incision but does not necessarily contact the bone along the length of the plate. This technique limits the disruption of periosteal blood supply that is seen in conventional plating techniques as the fixation is through the locking screws, thereby not necessitating compression of the bone to the plate for stability [31].

2.4.3. Static and Dynamic Fixation

Static fixation is the rigid fixation of a plate or fixture to bone or bone fragments eliminating all exposure of forces to the fracture site. The reasoning behind using static fixation over dynamic is that the elimination of all forces on the fracture allows the newly formed bone/callus to grow unaffected eliminating the possibility of ineffective growth or even re-fracture.

Dynamic fixation is the fixation of fractured bone to a device which allows the movement of the fractured bone. It is generally accepted that when a fracture is treated with a fixation device, dynamisation of the fixation accelerates formation of the bony callus by transferring parts of the functional load to the broken bone stimulating normal locomotion [32].

3. Material and Methods

3.1. Introduction

3-D image modelling and analysis is a very powerful tool in the medical field as doctors, surgeons and clinical engineers can convert CT scans into 3-D models allowing better visualisation of specific areas of interest. From these 3-D models surgeries can be planned, patient specific implants can be constructed and internal organs and structures can be visualised and exported to Finite Element Analysis (FEA) and rapid prototyping (RP) programs. This not only reduces operating time but also allows for more effective implants and treatment methods to be planned and produced before surgery allowing for better treatment, ultimately providing a reduced recovery period and improved healing. This section details the clinical trial procedure, biomaterial scaffold technology and describes the material and methods used to record the data required, carry out analysis on external stimulation factors using gait and FEA and also how the morphological changes were measured.

3.2. Clinical Scaffold Technology

The purpose of synthetic scaffolds is not to permanently replace the bone tissue; instead, the scaffolds are used as ‘intermediate phase’ implants. The scaffold should work as a medium to stimulate bone growth and encourage in the bridging of the fracture gap. The ideal scaffold for bone regeneration should have the following properties [34]:

- It should act as a three-dimensional template for bone regeneration.
- Resorption kinetics should be equal to the bone repair rate to facilitate load transfer to developing bone.
- The by-products produced should be non-toxic and easily excreted by the body.
- It should be biocompatible and promote cell adhesion (osteo-conductive) and cell activity (osteo-inductive).
- It should create a stable interface with the host bone without the formation of scar tissue.
- It should offer mechanical properties similar to the host bone.
- It must tolerate sterilisation according to the required international standards for clinical use.
- Optimally custom-fit shapes to fill defects would be produced [1].

Polymers are the most common organic materials and are biocompatible, degradable, have good processability and therefore have a great potential for scaffold materials. Some polymer types exhibit an even lower elastic modulus in comparison to bone and therefore are too flexible for load bearing solutions although the incorporation of ceramic constituents into the polymer can help to address this problem [35].

3.3. Clinical Trial Procedure

A group of 21 skeletally mature adult sheep were entered into the test after being deemed healthy and suitable by a Veterinary Doctor at Keldur. The sheep were kept at all times at the Keldur facility and cared for and observed by the staff there. They were kept in a holding pen at all times to allow close observation and to reduce the possibility of sustaining more injury than that induced at the beginning of the trial.

The 21 sheep had a single fracture induced to the right hind tibia diaphysis in which a 25 mm section of bone was removed. In 7 of the sheep, no scaffold was inserted into the bone gap, in another 7 of the sheep a prototype internal clinical scaffold produced by GENIS was inserted into the bone and in the remaining 7 sheep an already available internal clinical scaffold was inserted into the bone. In all cases a LISS internal fracture fixation device was applied to the bone to secure both the proximal and distal sides of the fracture, the wound was closed and a plaster cast applied to the leg to prevent the flexion and extension of the leg and to provide support to allow the sheep to walk. The operation procedure is shown below in figure 3.1.



Figure 3.1. a, b, c. Operation procedure showing resection of bone (a), placement of fixture device and scaffold (b) and attachment of fixture device (c).

After the fracture had been induced, the fixation applied and the operation completed all the sheep were left for 20-21 weeks in which the tibiae were left to heal. X-rays were taken of the sheep legs during this time to allow observation of the fracture fixation and ensure the bone was healing in such a way as to not cause distress to the sheep. During the observation period the sheep were free to walk as normal in the holding pen.

After 20-21 weeks the tibiae were removed from the sheep. An incision was made above the leg, where the main leg artery and a vein were located. Intravenous tubes were placed inside the artery and vein and saline was pumped through to clean the veins of the leg. Formalin (formaldehyde diluted in water) was then pumped into the leg using a peristaltic pump to “freeze” the leg and to stop the deterioration of the biological tissue. The sheep was then sacrificed and the leg was amputated at the tibia- femur joint and above the tuber calcaneus and tarsus joint (see section 2.2), the tibia was then removed. The left hind tibia was also removed in some cases to provide a contralateral specimen. The residual flesh and the fracture fixation device were then removed from the specimen and the tibiae were submerged in formalin and taken for computed tomography (CT) scans (process is shown in figure 3.2).

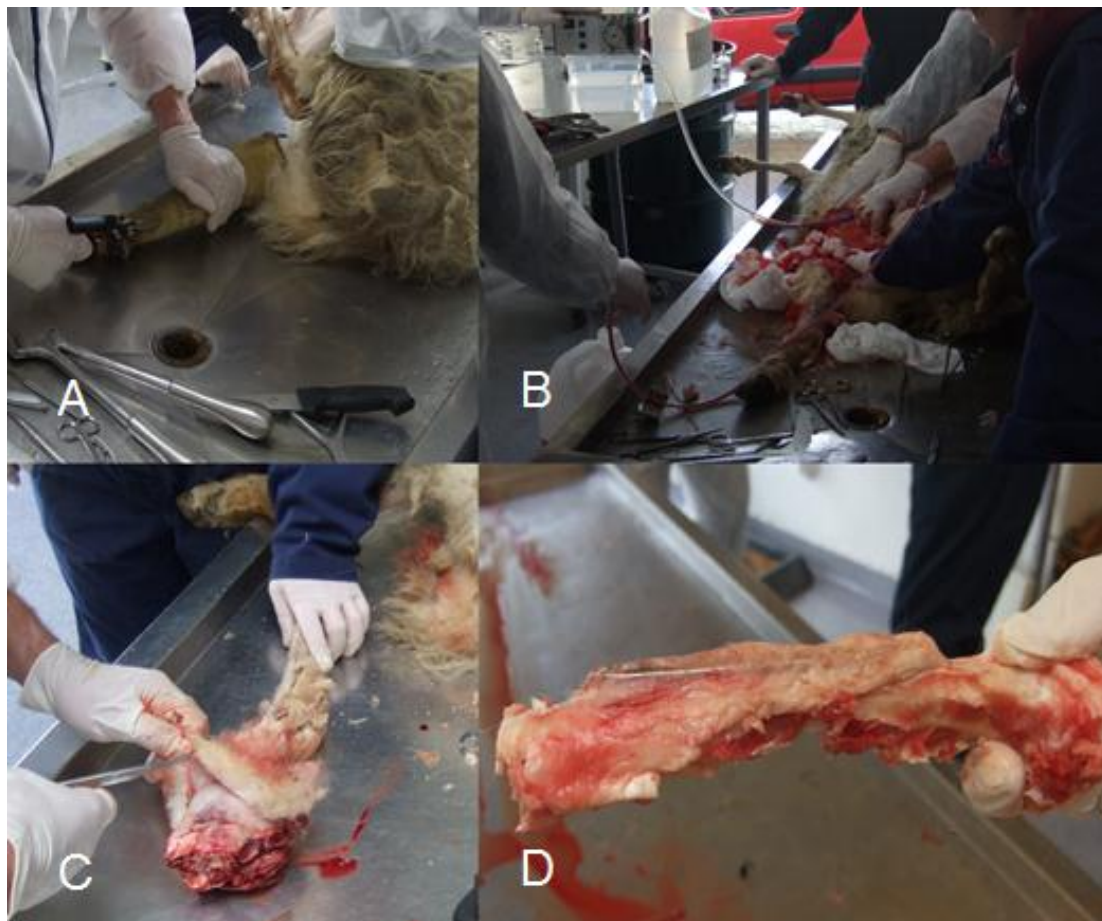


Figure 3.2. a, b, c. Removal Procedure showing removal of cast (a), insertion of formalin (b), removal of leg (c) and removed tibia with fracture plate (d)

3.4. Gait

Some of the sheep appeared to be walking normally when observed visually, but to accurately observe the walking pattern the gait of the sheep was measured using GAITFour [36]. The standard GAITFour electronic walkway (figure 3.3) automates spacial, pressure and temporal measurements. The device contains eight sensor pads encapsulated in a roll up carpet to produce an active area 24 inches (61 cm) wide and 192 inches (488 cm) long. In this arrangement the active area is a grid, 48 sensors by 384 sensors placed on 0.5 inch (1.27 cm) centres, totalling 18,432 sensors. As the test subject ambulates across the walkway, the system captures the geometry and the relative arrangement of each footfall as a function of time. The application software controls the functionality of the walkway, processes the raw data into footfall patterns, and computes the temporal and special parameters [36]. These parameters are used in several calculations carried out by the program to give various results of both temporal and special readings. Recall from earlier in the chapter that it is the rear right hind leg that has the induced fracture. The stride length, mean stance time and peak pressure were measured and used to determine to what extent the sheep are using the injured limbs, this was taken into consideration as external factors such as locomotion can have an effect on the remodelling process. A total of three sheep were used (two involved in the trial, and one unaffected sheep) each completing two walks.



Figure 3.3. GAITFour setup showing Mat and sensor pads (left hand side of mat)

3.5. Spiral Computed Tomography

A generic block diagram of a CT scanner is shown in figure 3.4 below, it can be argued that the actual system architecture for different commercial scanners may deviate slightly from the diagram but the general functions of these scanners are very similar.

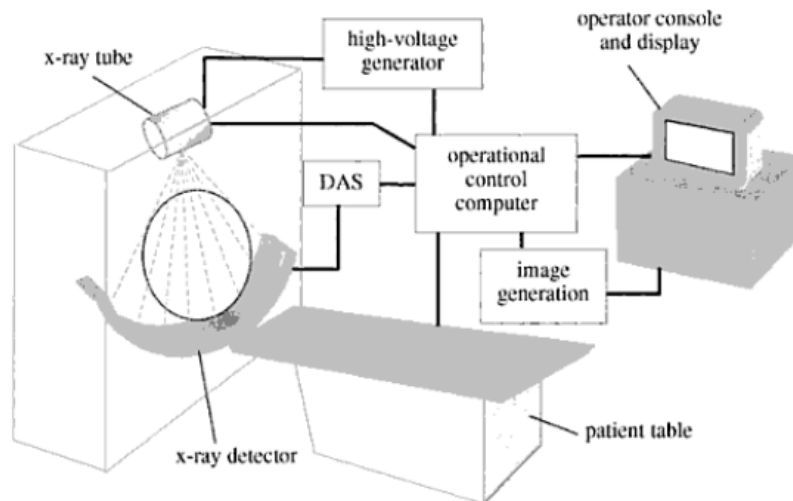


Figure 3.4. Block diagram of a CT scanner [37]

During the scanning phase a fan shaped beam is moved around the body while the body is moved through the beam area at a continuous velocity. Pitch value is the distance the body is moved during one beam rotation, expressed as multiples of the x-ray beam width or thickness. With the increased pitch rate the x-ray beam moves quickly along the scan body reducing the scan time to cover a specific body volume which reduces the dose of radiation, it also however reduces the detail in the data which can reduce the quality of the image produced.

Image reconstruction is the phase in which the scan data set is processed to produce an image which is digital and in the form of a matrix of pixels. Filtered back projection is the reconstruction method used in CT and the term 'filtered' refers to the use of the digital image processing algorithms that are used to improve image quality or to change image quality characteristics such as detail and noise.

Figure 3.5 shows the formula used to calculate the CT number or Hounsfield unit (HU) for each pixel. The HU numbers are calculated from the x-ray linear attenuation coefficient values for each individual tissue voxel. It is the attenuation coefficient that is first calculated by the reconstruction process and then used to calculate the HU number values. Water is the reference material for HU numbers and has an assigned value of zero. Tissues or materials with attenuation (density) greater than water will have positive HU numbers. Those that are

less dense will have negative HU numbers. X-ray attenuation depends on both the density and atomic number (Z) of materials and the energy of the x-ray photons [39].

The diagram illustrates the calculation of a CT number from a tissue voxel. On the left, a yellow box labeled 'TISSUE VOXEL' contains the symbol μ and is labeled 'ATTENUATION COEFFICIENT'. Below it, 'DENSITY' and 'Z' are indicated with arrows pointing to the μ box. In the center, the formula is shown:
$$\frac{\mu_{\text{Tissue}} - \mu_{\text{H}_2\text{O}}}{\mu_{\text{H}_2\text{O}}} \times 1000 =$$
 On the right, a grey box labeled 'IMAGE PIXEL' contains the text 'CT NUMBER'.

Figure 3.5. Calculation of CT or Hu number [39].



Figure 3.6. Scanning of Removed Tibia

3.6. Medical Image Processing

3.6.1. Importing Data

Image slices obtained from the spiral CT scan are exported in the DICOM (Digital Imaging and Communications in Medicine) format, a standard for handling, storing, printing, and transmitting information in medical imaging. The DICOM image files generated by the CT are coded according to the Hounsfield scale [39].

For the reconstruction of the scan body, the DICOM image files generated from the CT scan are imported into MIMICS [40]. When scanned the CT scanner breaks down the 3-D body into a 'stack' of 2-D slices, when imported into MIMICS, the software does the reverse by

‘stacking’ the 2-D slices to create the 3-D body. Stacking involves placing all the 2-D image slices next to each other in the correct order forming the 3-D model (figure 3.7).

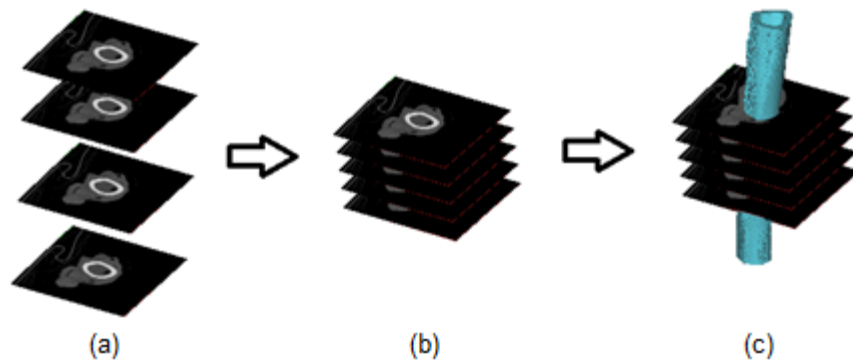


Figure 3.7. (a) 2-D DICOM files obtained from CT scan, (b) Stacked DICOM files in the MIMICS program, (c) Resultant 3-D model created in MIMICS from the stacked DICOM files.

3.6.2. Segmentation and Modelling

The MIMICS software creates models based on the HU values within the CT images. MIMICS has the flexibility to create models from any geometry distinguishable within the scanned data by grouping together similar HU values [40]. Segmentation is achieved through various stages of thresholding, region growing and 3-D model creation (figure 3.8).

Thresholding is the process of identifying certain regions and materials to be separated from the scan data and grouped together using the HU values assigned to each pixel. During thresholding a certain region of interest is identified using a range of HU values for the tissue that is to be segmented. Every pixel in the scan area with an HU value which lies in this interval is marked, if a pixels HU value does not fall within the specified interval then it is not included in the mask.

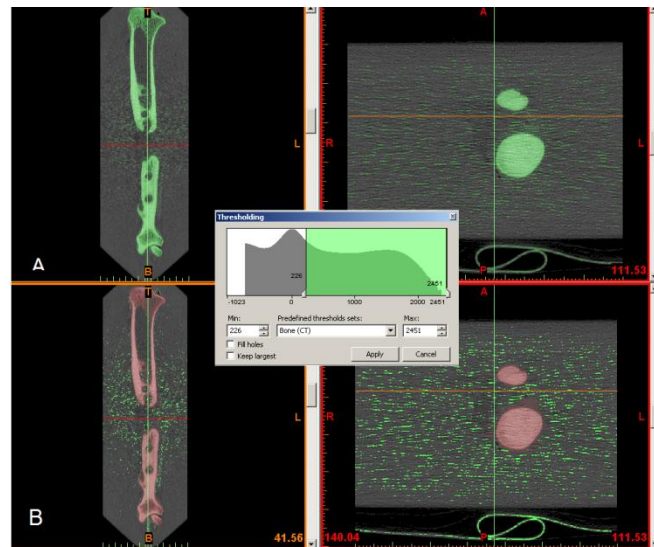


Figure 3.84. Segmentation Process Showing Thresholding (A) and region growing (B) with segmentation selection Process shown in the middle.

Once thresholding has been completed, the marked pixels from the material or area of interest can now be ‘grouped’ together, a process called region growing. When any highlighted pixel is selected, the software groups together all the connected highlighted pixels producing a new highlighted section of pixels which lie in the selected interval. This can be bone, fat, muscle or a certain area of interest, i.e. the knee or hip, which would then undergo repeated region growing to separate further the different areas of interest. Depending on the scan quality or the separation success, the highlighted pixels or ‘mask’, may have to be edited. Editing a mask eliminates pixels which the region growing process has included in the mask which are unwanted. This has to be done sometimes to separate materials that are joined in the scan but have to be separate masks and have to have region growing applied separately. Mask editing can also be carried out to add pixels to a mask if they have been eliminated from the mask during region growing, or if extra material is required to be added, i.e. for implants or surgical planning.

With the correct volumes masked, the materials or areas separated in the various masks can now be converted, using the MIMICS software, into 3-D objects. The objects can be further edited in 3-D mode to ensure only the desired volume is modelled and can then be exported to various external programs for further analysis (figure 3.9).

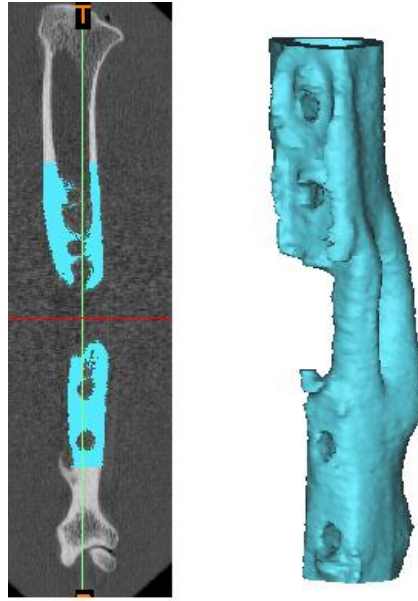


Figure 3.9. Edited mask for region of interest (left), 3D model constructed from mask (right)

3.6.3. Morphological Changes

The CT scans of the two groups of specimens (7 specimens in each group) containing the two scaffold types were imported into MIMICS and then segmented. Group A was omitted from the scaffold analysis section as it contained no scaffold. Initially the complete specimen (bone material and scaffold) was identified from the scan data, the removed bone section was segmented, then the scaffolds were edited from the new bone material and masked separate from the additional surrounding materials.

Control scaffolds for both groups were also acquired, scanned and masked appropriately. Volumes of the various masks used were calculated by summing the volume of all the voxels (pixel cube volume) that have been identified in the mask. The mean density for a mask was calculated by summing all the densities of the voxels that were highlighted during the mask segmentation. The sum is then divided by the number of voxels in the mask giving the mean density of the mask volume. Density regions in masks can be assigned different colours which can then be used to show the density distribution throughout the model.

3.6.4. Absolute Screw Movement

Screw movement during fixation can lead to screw pull out and can also affect the remodelling of the bone by introducing a level of dynamic fixation (figure 3.10). Measurements were taken from reference points created from the CT scans in MIMICS and compared to measurements taken from a specimen fixation device using the same reference points. Measurements of the screw locations pre and post op were taken and differences in the measurements were summed to give an absolute screw movement value for each specimen.



Figure 3.10. Measurement of screw movement showing typical scan after 2 weeks (left) and extreme case after 17 weeks (right).

3.6.5. Proximal and Distal Density Loss

The process of remodelling can be affected by mechanical stimulation. As the test specimens had an induced fracture gap with fixation device applied over the span of the gap, mean density losses were measured in the proximal and distal sections to determine if one of the sections retains more density than the other during the remodelling process which could be an indication of varying levels of mechanical stimulation. The proximal and distal sections were masked individually and the mean density was recorded pre and post operation to determine total density losses in the two sections.

3.7. Finite Element Modelling

3.7.1. Finite Element Method

The finite element method (FEM) or FEA is a computational technique which approximates solutions of boundary value problems allowing for simulations on models using a theoretical method. Figure 3.11(a) shows an area which represents a boundary value problem of interest. In the two dimensional case the shape represents a single field variable $\phi(x,y)$ which, in order to provide a solution to the analysis, has to be determined at every point $P(x,y)$. A small triangular element that encloses a finite sized section of the area of interest is shown in figure 3.11(b). The vertices of the triangular element are numbered 1-3 to indicate that these points are nodes. A node is a specific point in the finite element at which the value of the field variable is to be calculated.

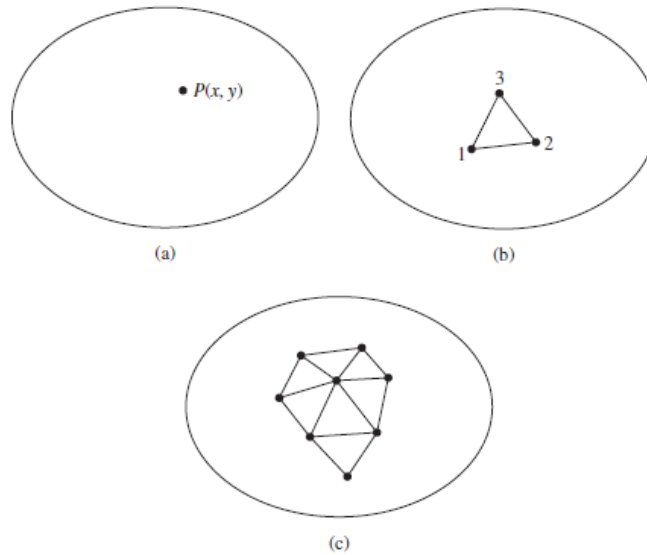


Figure 3.11. (a) A general two-dimensional domain of field variable $\phi(x,y)$. (b) A three node finite element defined in the domain, (c) Additional Elements showing a partial finite element of the domain [41].

The values of the field variable computed at the nodes are used to approximate the values at the non-nodal points by interpolation of the nodal values. For the three node triangle example the field variable is defined by the approximate relation in equation 1 [41].

$$\phi(x,y) = N_1(x,y)\phi_1 + N_2(x,y)\phi_2 + N_3(x,y)\phi_3 \quad (1)$$

Here, ϕ_1, ϕ_2, ϕ_3 , are the values of the field variables at the nodes and N_1, N_2, N_3 are the interpolation functions also known as shape functions or blend functions. These functions are predetermined, known functions of the field variable within the infinite element. In general, the number of degrees of freedom associated with a finite element is equal to the product of the number of nodes and the number of values of the field variable that must be computed at

each node. As shown in figure 3.11(c) every element is connected at its exterior nodes to other elements. The finite element equations are formulated that, at the nodal connections, the value of the field variable at any connection is the same for each element connected to the node [41]. Using this technique volume meshes can be created for complex models allowing for repeated analysis which could be otherwise expensive, time consuming or destructive.

3.7.2. Post-Operative Model

In order to conduct FEA analysis on the post-operative model to determine external stimulation factors, a fixation plate (figure 3.12) was designed in Autodesk Inventor replicating the fixture plate used in the setup procedure. This plate was imported into MIMICS and using relocation techniques the plate was positioned on the tibia in the location shown in the x-rays taken post-op (figure 3.10 pg. 19). The induced fracture and screw holes were reproduced on a control specimen using mask and region editing techniques to replicate the post-operation setup.

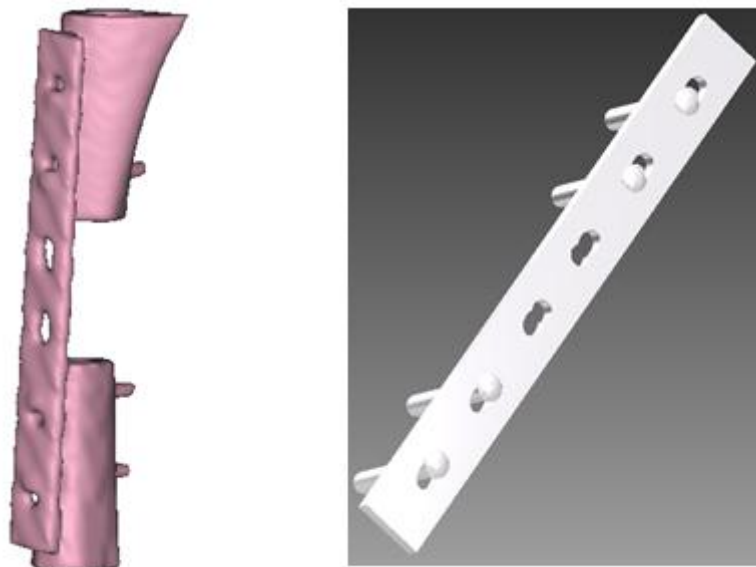


Figure 3.12. (Left) Post-operation setup, fracture plate assembly and tibia after induced fracture and plate application operation. (Right) Fracture plate and screw assembly which was imported into mimics.

3.7.3. Meshing in 3-Matic

The process of representing a physical domain with finite elements is referred to as meshing with the resulting set of elements known as the finite element mesh. 3-Matic is a software package which allows volume meshing on anatomical models. The volume to be meshed from MIMICS was imported into 3-Matic [40] and the volume refined with smoothing of the model to eliminate irregular edges and surfaces to make the meshing process less complex. Reduction of triangles, automatic re-meshing and quality preserving were carried out on the volume to produce a volume mesh of the model (figure 3.13).

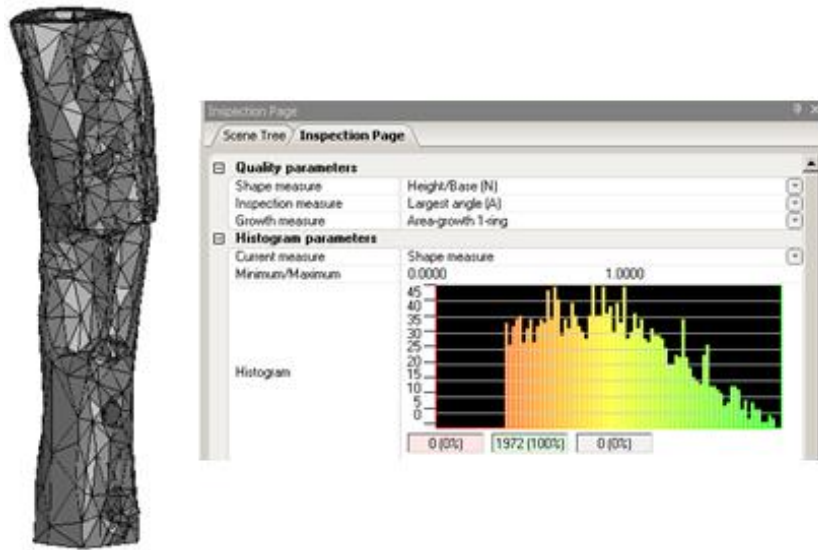


Figure 3.13. (Left) Meshed model and (right) inspection tree with mesh information.

3.7.4. Material Assignment

Before finite element analysis can be carried out on the volume, material properties must be assigned. The mesh created in 3-Matic is then exported back to MIMICS where the material properties can be assigned to the mesh. Each material can be assigned an absolute density value, E-modulus and Poisson coefficient depending on the HU value from the CT scan or material properties can be assigned to specific regions if no CT data exists or the CT data is undesired. The apparent density for the bone sections are calculated in each pixel using equation 2 [42]

$$\text{Apparent Density } \rho_a \left(\frac{g}{cm^3} \right) = 1 + \frac{HU}{2564} \quad (2)$$

The apparent densities are assigned to the model in 10 different HU value regions. The material properties were assigned to the fixture plate and screws from data obtained from the manufacturer (figure 3.14).

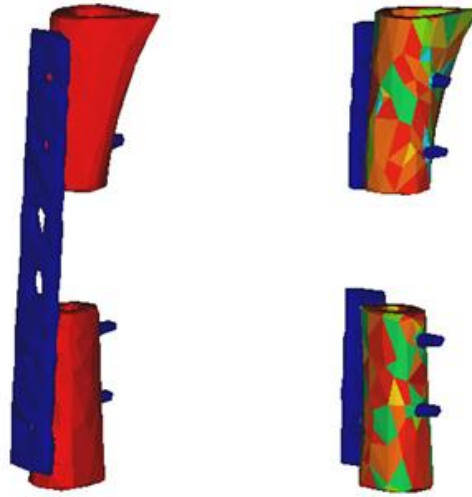


Figure 3.14. (Left) Material Assignment of homogeneous bone densities and (Right) proximal and distal sections with 10 density regions both shown with fracture plate assembly.

3.7.5. Contact Regions

The model with assigned material properties was then imported into ANSYS. After the model had been imported, the skin components are checked for ‘bad surfaces’ or incorrect modelling, once the initial geometry has been verified, contact regions have to be identified. Regions of contact between bone, plate and screws have to be identified and allocated frictional values to replicate the real life interaction between the volumes. Frictional coefficients of 0.5 were applied to areas of contact between the screws and bone. The contact areas between fracture plate and bone were allocated a non-frictional value as ideally there should be no or minimal friction between the volumes (figure 3.15).

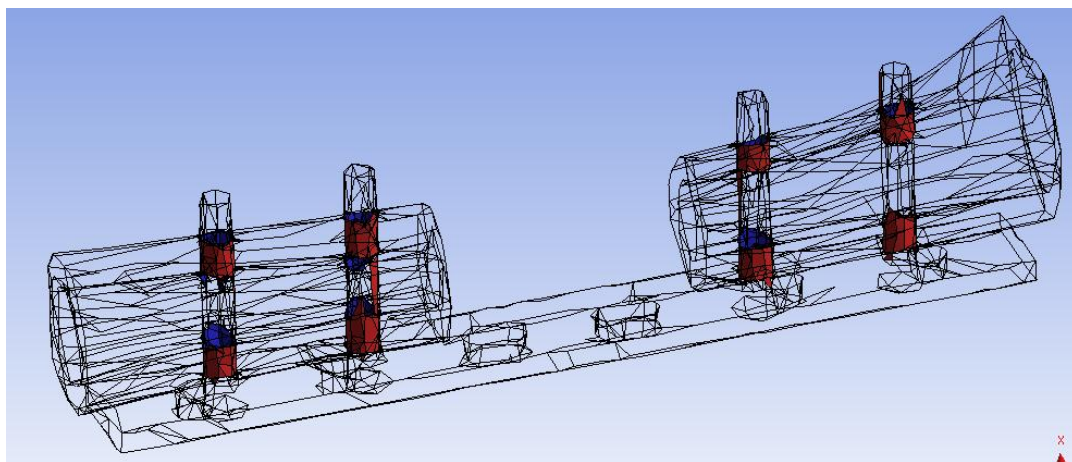


Figure 3.15. Post-op model shown with highlighted contact regions between screw and bone.

3.7.6. Application of Forces and Fixtures

The forces and fixtures can now be applied to the model. Forces were applied proximally and distally to the cross-sectional faces of the bone in opposing directions to simulate the free movement of both sections whilst the plate was fixed at the centre to properly fixate the model. To simulate normal locomotion (walking, running, sudden movements) a force of 877N, 300% of the normal body weight of a skeletally mature sheep was applied to the model both proximally and distally (figure 3.16) [43].

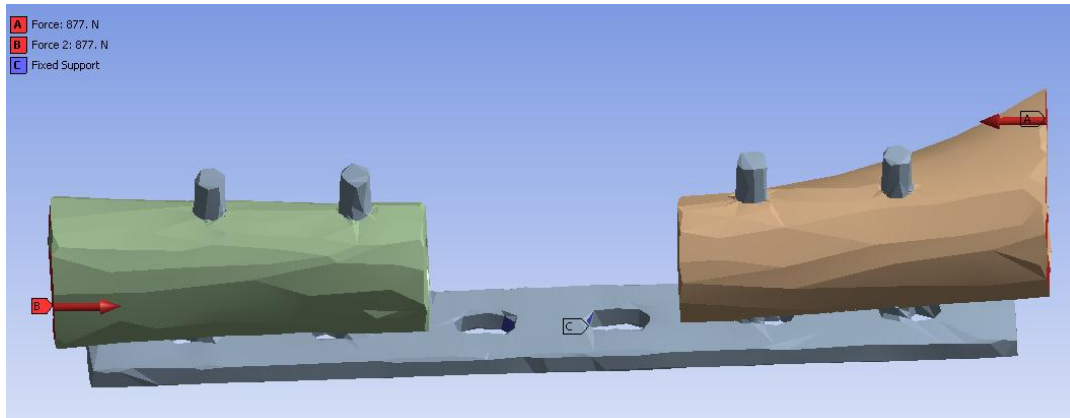


Figure 3.165. (A) Forces Applied to Model Proximal, (B) Distal with (C) fixed support at centre screw holes.

3.8. Protocols and Calibration

To ensure all data would be of the same quality and clarity, scan protocols were put in place. Each time the specimens were scanned the same area of interest and setup of the scanner was used. Pixel size was set at 0.137 mm^2 with a slice size of 512 by 512 pixels and a slice thickness of 0.67 mm. The gantry was set at 0° and each scan produced on average 680 slices depending on the length of the specimen which gave a total data set size of $512 \times 512 \times 680 \times 12 = 2.14 \text{ GB}$. The same protocol was used when scanning the control specimens.

During segmentation the dimensions for the segmentation volumes were standardised allowing for accurate comparisons between specimens. As the fixture device used was identical between specimens a distance of 20 mm proximal and distal of the external screws was used as the extremities of the volume used for analysis. For the removed section of bone, distances of 10 mm from the internal screws were used to identify this region.

Calibration of the imaging quality and verification of the use of HU values to display density was carried out in a previous study [44] in which 3 different scanners were compared using a QUASAR (Quality Assurance System for Advanced Radiotherapy) phantom as the scan material. The calibration phantom body was carefully positioned on the scan bed and aligned

through the laser alignment marks on the phantom with either the CT suite room laser or the CT scanner laser. Calibration elements such as lung, polyethylene, water equivalent, trabecular and dense bone were placed in the phantom body to be scanned. Using a pre-determined protocol the phantom was scanned and results were analysed using MIMICS and excel. The study showed some variation between HU units and suggests using scanner specific customized HU intervals when studying bone and muscle density changes. Following these results, HU intervals for the CT scanner used were implemented in the analysis process to ensure accurate results.

4. Results

4.1. Introduction

This section documents all the results obtained during trials and analysis using the material and methods described in chapter 3. Group C specimen 21 was excluded from results section 4.3 as there was an extensive amount of artefacts in the scan which can affect the results and lead to inaccurate conclusions.

4.2. Gait

Section 4.2. illustrates the results of the Gait test used to determine if the sheep are using the injured leg which can affect the remodelling process.

4.2.1. Stride length

Below (figure 4.1) are the results for the sheep stride length which is one of the methods used to determine if the sheep are using the injured leg during locomotion.

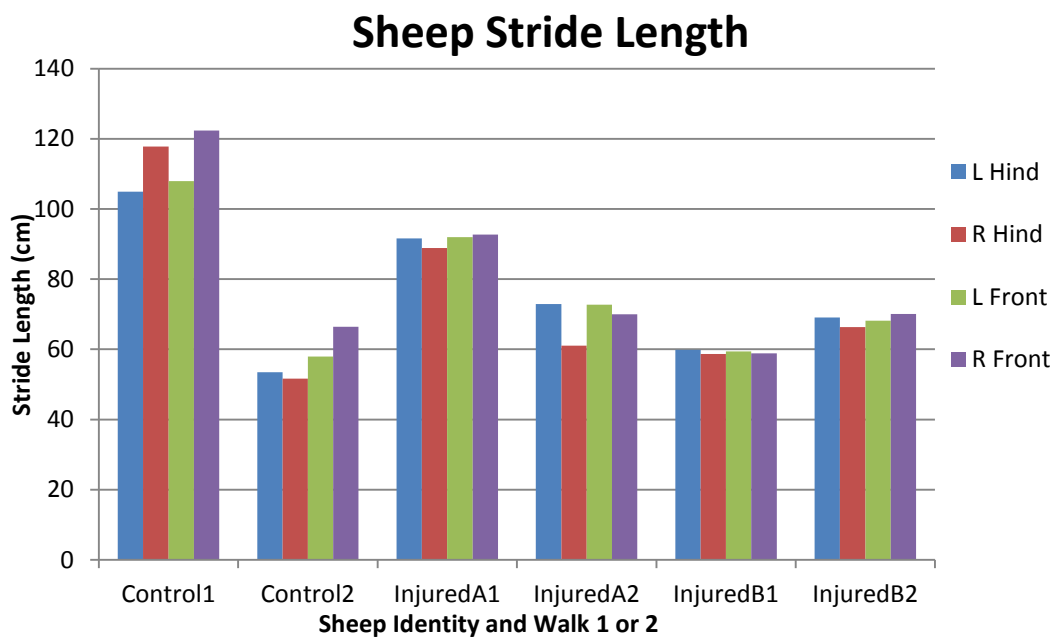


Figure 4.1. Both walks by all three sheep with the average stride length shown for all limbs during the walk.

The variation in stride lengths between sheep can be a result of different velocities during the walk. If a sheep is walking quicker the stride lengths will be larger than if the sheep was walking slowly. Small irregularities between rear leg stride lengths can be observed in all sheep walks and is no indication of a more favourable limb. From looking at these set of results it would appear the sheep have a regular gait pattern and present no abnormalities.

4.2.2. Mean Stance Time

Results for mean stance time for the sheep walks can be seen in figure 4.2. Mean stance time is another method to identify if the sheep have a normal locomotion cycle.

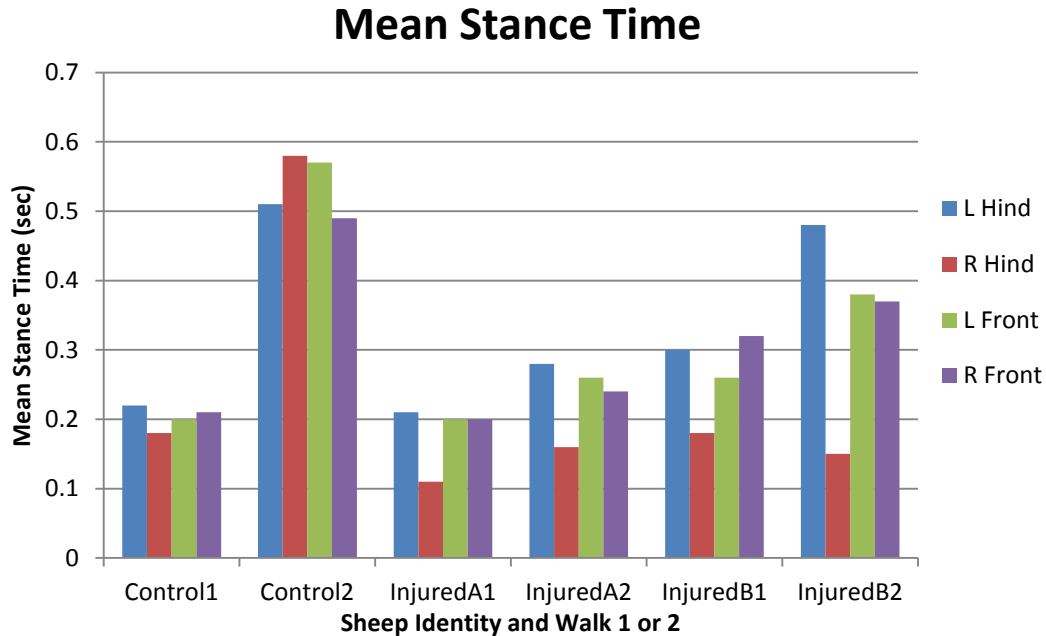


Figure 4.2. Average mean stance time shown for all specimen walks and for all limbs during the walks.

Following on from the previous mentioned velocity differences, a shorter stance time indicates a faster walk while a longer stance time indicates a slower walk. It can be observed from the injured sheep walks that all right legs have a shorter stance time than the left hind legs indicating a preference to spend more time on the left hind legs. It can be seen in the control sheep that a difference in stance times are visible between hind legs, this varies between both legs and so on average there is no real preference for one leg over the other.

4.2.3. Peak Pressure Index

Here we can see the results for the measured peak pressure per limb results. This is another method to determine if the sheep are using the leg normally during locomotion.

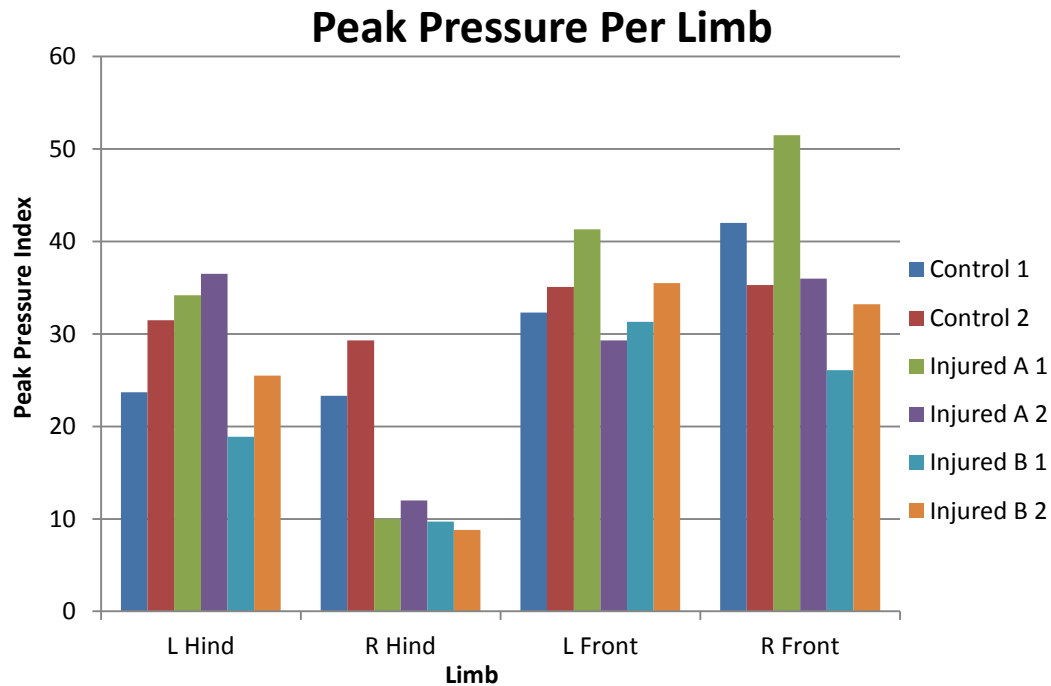


Figure 4.3. Average Peak pressure index shown for all sheep walks for all limbs during the walks.

It can be clearly seen from figure 4.3 that the injured sheep are applying a reduced amount of pressure to the rear right limb, this shows that although the sheep may appear to have a normal gait cycle, the mechanical stimulation achieved from normal gait would be reduced due to the reduced amount the sheep utilises the limb.

Figure 4.4 overleaf is used to confirm the sheep are constantly applying less weight to the leg and shows a complete walk for sheep C2.

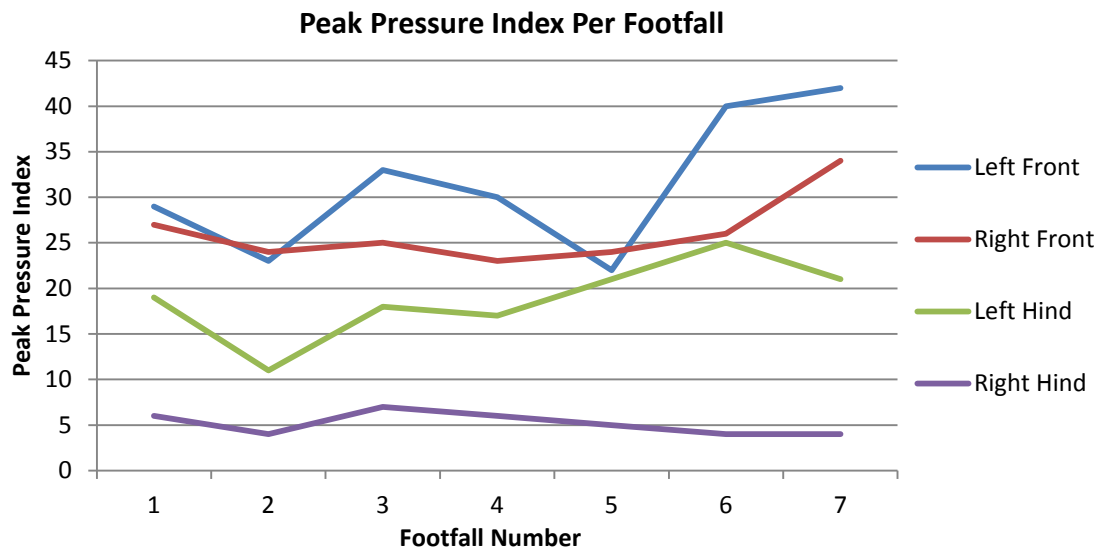


Figure 4.4. Peak Pressure index per footfall for a complete walk of injured sheep C2.

Figure 4.4 displays an entire walk for injured sheep C2 showing the peak pressure index. The constantly reduced applied pressure illustrates that the sheep is applying a reduced pressure throughout the entire walk.

4.3. Morphological Changes in Bone and Scaffold

Section 4.3 displays the morphological changes in both the new bone material and scaffold volumes focusing on density and volume growth while also displaying density distribution and comparisons to the removed bone control section.

4.3.1. Scaffold Volume

Figure 4.5 overleaf displays the scaffold volumes for groups B and C which is used to quantify the growth of the new material in the scaffold.

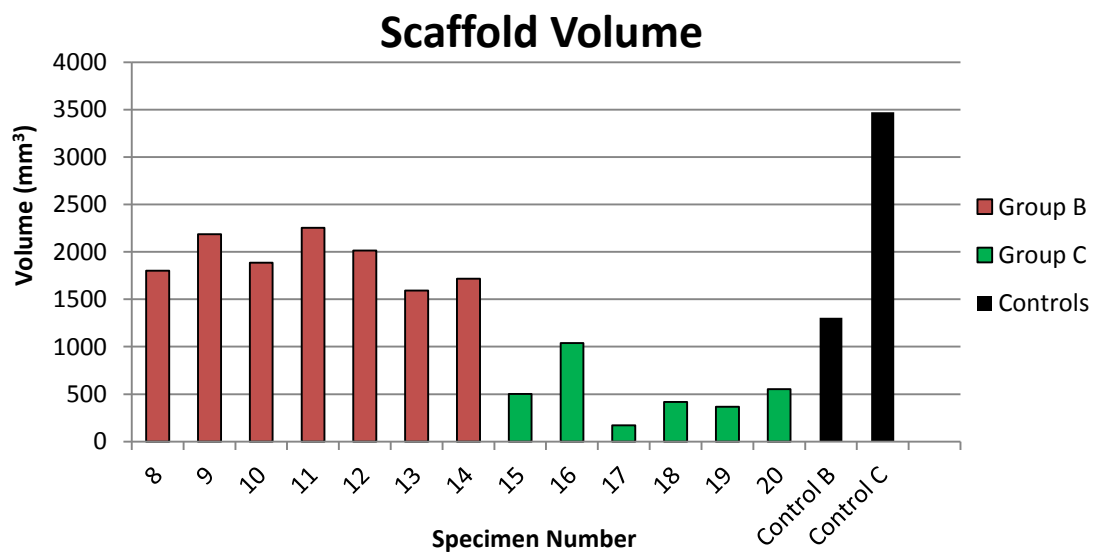


Figure 4.5. Scaffold Volumes from groups B and C and respective control scaffolds.

Figure 4.5. shows that all group B specimens have an increased level of volume when compared to the group B control scaffold with an increase in volume ranging from 22% - 72%. Drastic reductions can be observed in group C scaffold volume when compared to group C control scaffold with reductions ranging from 334% - 2013%. The reduction in group C volume could be due to deterioration of the scaffold during the remodelling period or absorption on the scaffold by the surrounding tissue.

4.3.2. Scaffold Mean Density

Scaffold mean density is measured here to illustrate the quality of the new material formed in terms of density when compared to the other group, the control scaffold and also the mean bone control density shown at the top of the graph as a dashed blue line.

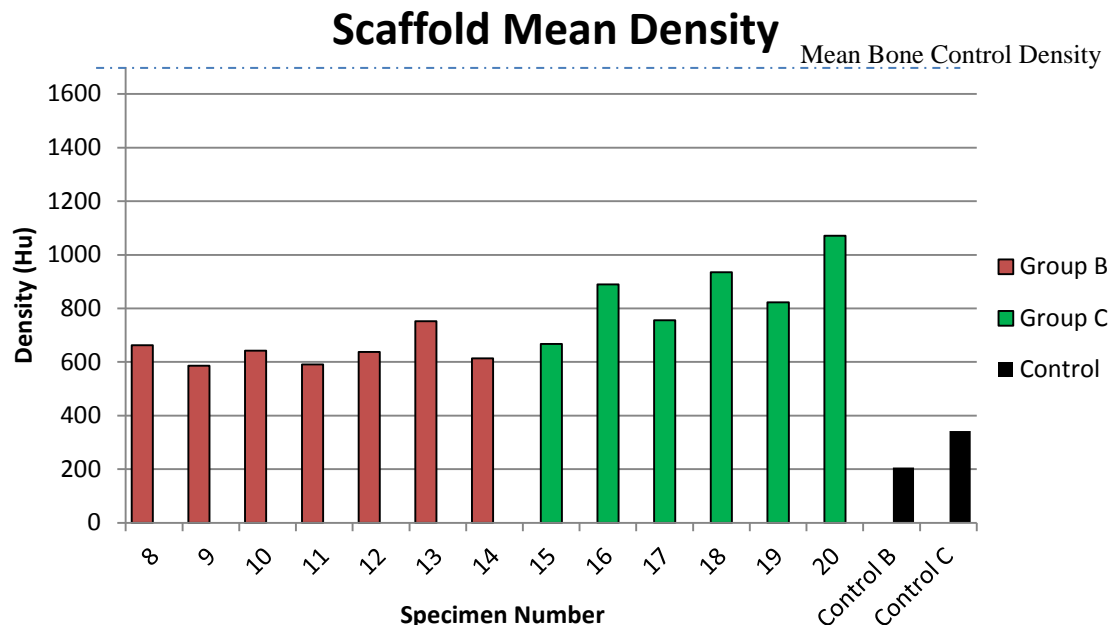


Figure 4.6. Groups B and C scaffold mean density and control scaffolds and the average mean control density.

It can be seen in figure 4.6 that all scaffolds present a significant increase in mean density when compared to the control scaffolds. Observed increase in density in group B ranges from 283% - 364%, while in group C the increase is from 194% - 312%. The increase in density shows that the new material has formed inside the scaffold area is increasing in density which indicates the scaffold can promote and sustain new material formation throughout its structure.

4.3.3. Scaffold mean Density and Volume Correlation

Scaffold mean density and volume correlation is used to illustrate possible trends between the groups to identify trends forming between groups which may indicate if one of the groups is promoting and sustaining new material formation within the structure better than the other.

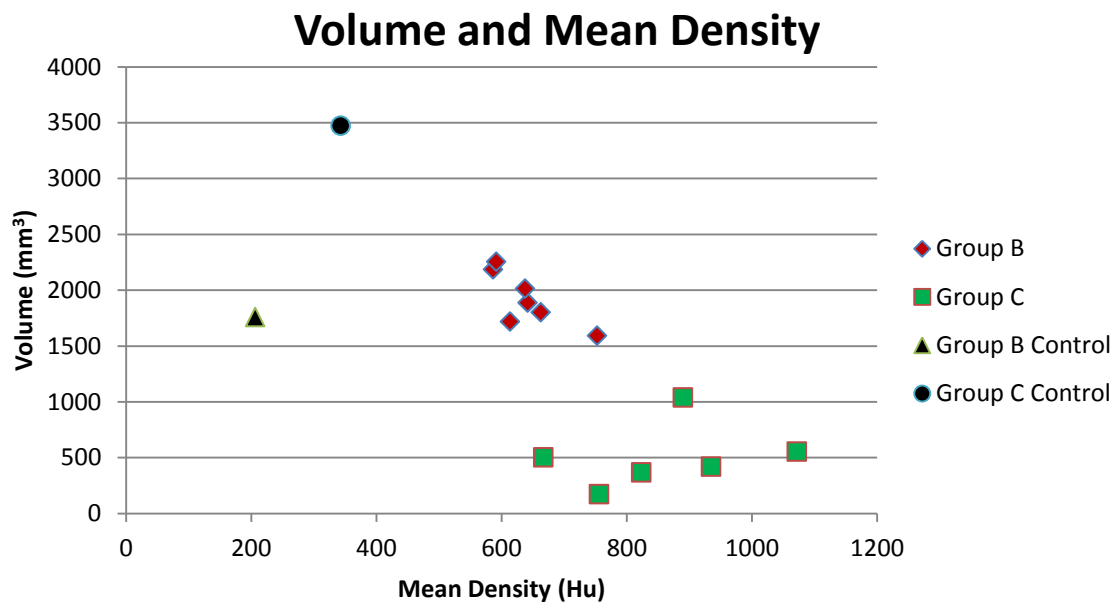


Figure 4.7. Correlation between scaffold types and controls showing mean density and volume for all groups.

From figure 4.7 it can be observed that there is a difference in trends between the two scaffold groups. Group B specimens have a lower mean density than group C specimens, while also displaying a higher volume than group C specimens. From these results it is difficult to show one scaffold is performing superior to the other as both have displayed performance qualities required from a scaffold.

4.3.4. Scaffold Density Distribution

Density distribution of the scaffolds is performed to determine how similar the compositions of the scaffolds are to both the control scaffolds and also the control bone section. This displays if the scaffolds are increasing the density throughout the bone material density range (220 HU – 2976 HU) or if the material is promoting growth only to a certain value.

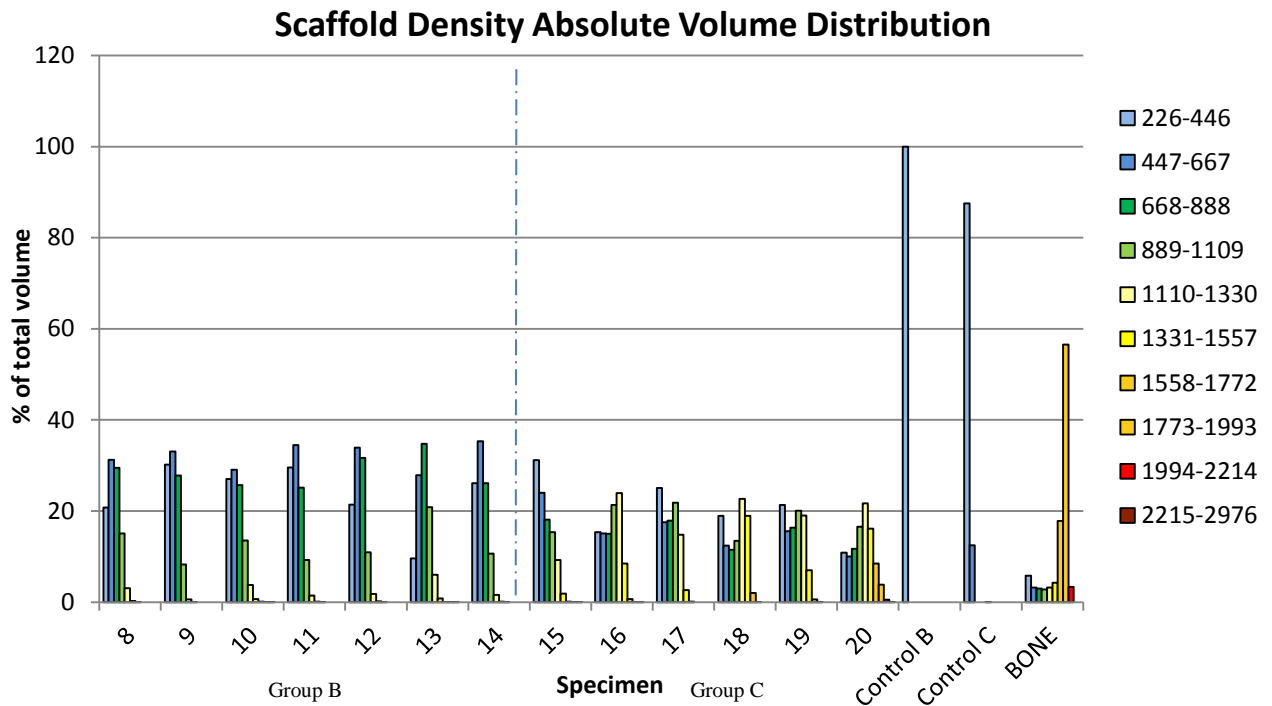


Figure 4.8. Density regions displayed as a percentage of total volume of scaffold, control and control bone specimens with the densities given in Hounsfield Units.

The results show that both groups have a large majority of the material density in the range 220 – 435 HU with an almost opposite distribution observed in the control bone with 78% of densities higher than 435 HU making up the control bone volume. Both specimen groups show an increase in distribution in densities higher than those found in the control scaffolds. While this displays the scaffold groups are dissimilar to the control bone in terms of density distribution, the increase in density compared to the control scaffold shows there is remodelling occurring throughout the scaffold volume.

4.3.5. Scaffold Density Distribution Slices

To observe the density distribution of the material inside the scaffold volume and to allow for comparisons between specimens, control scaffolds and control bone density distributions, cross-sectional slices were recorded displaying the density regions throughout the structures.

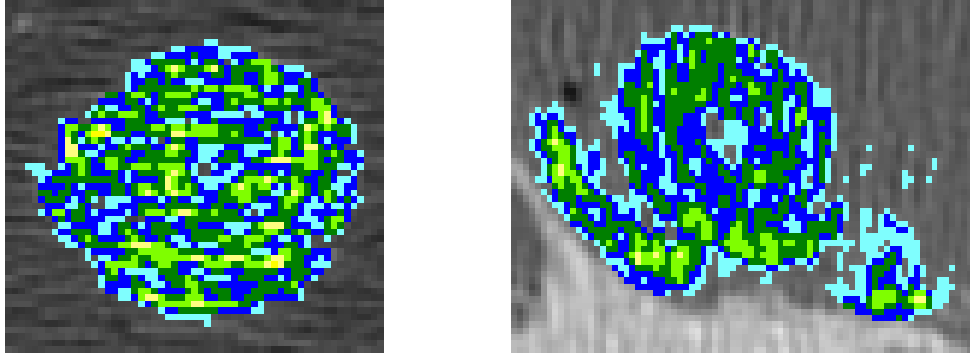


Figure 4.9. a, b Two specimen slices (left to right a and b)

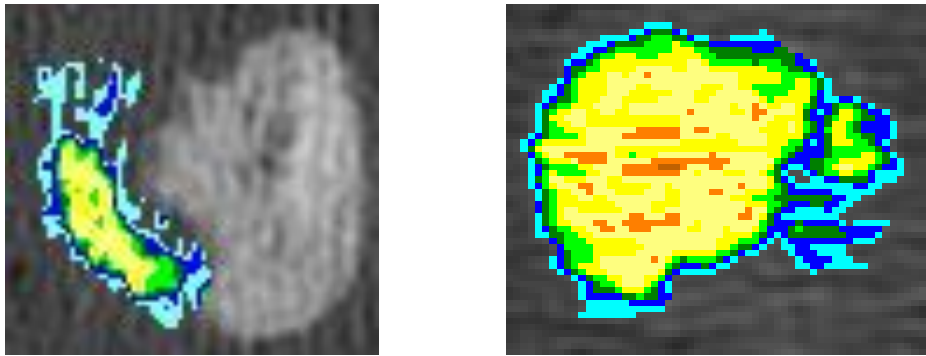


Figure 4.10. a, b Two specimen slices (left to right a and b).

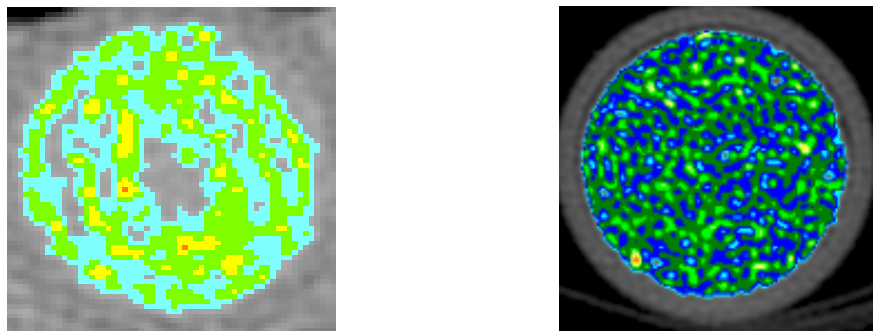


Figure 4.11.a,b Control Scaffolds group B and C left and right respectively

Table 4.1. Density regions for Scaffold Segmentation

Density Range (Hu)
101-200
201-300
301-400
401-500
501-640
641-741
741-841
841-1506

Some of the specimens displayed an even distribution of low density materials throughout the scaffold (figures 4.9 a, b). Both groups displayed specimens that retained the circular cross-section (4.9 a), while both groups also contained specimens which have deteriorated and failed to retain the circular cross-section (4.9 b, 4.10 a, b). Both control scaffolds displayed an equal distribution (4.11, 4.12) of the various density regions (table 4.1).

4.3.6. New Material Volume

New material is classed as any material in the resection volume not classed as scaffold material as is measured to determine the amount of new material formed in the resection volume. This gives an indication of the group's ability to promote and sustain new material formation.

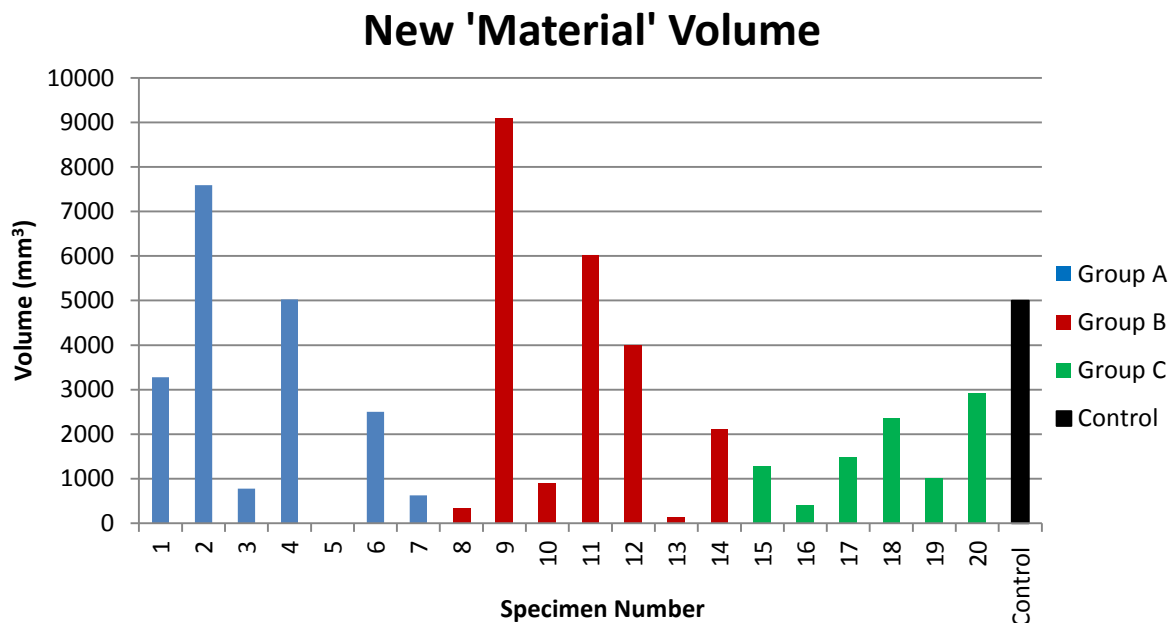


Figure 4.12. New material volume for all specimens from all groups and the average bone volume from the same removed section from the contralateral specimen.

All groups display varying levels of new material volume as shown in figure 4.12 while specimens 2, 9 and 11 show an increased volume compared to the removed bone indicating that this may be the formation of a callus growth. Group B possesses the highest percentage increase in volume (specimen 9) (182%) and also the highest percentage loss in volume specimen (specimen 13) (3874%) while in group A specimen 5 suffered a plate fracture and presented no new material, possibly as a result of the plate fracture. Group B had the highest average percentage of the control volume with 65%, group A had the second highest at 57% and group C had the lowest average percentage of the control volume at 37%.

4.3.7. New Material Mean Density

The mean density of the new material can be an indication of how successful the remodelling process has been in terms of the new material being of a similar density to the control bone which is shown at the top of the figure as a dashed line.

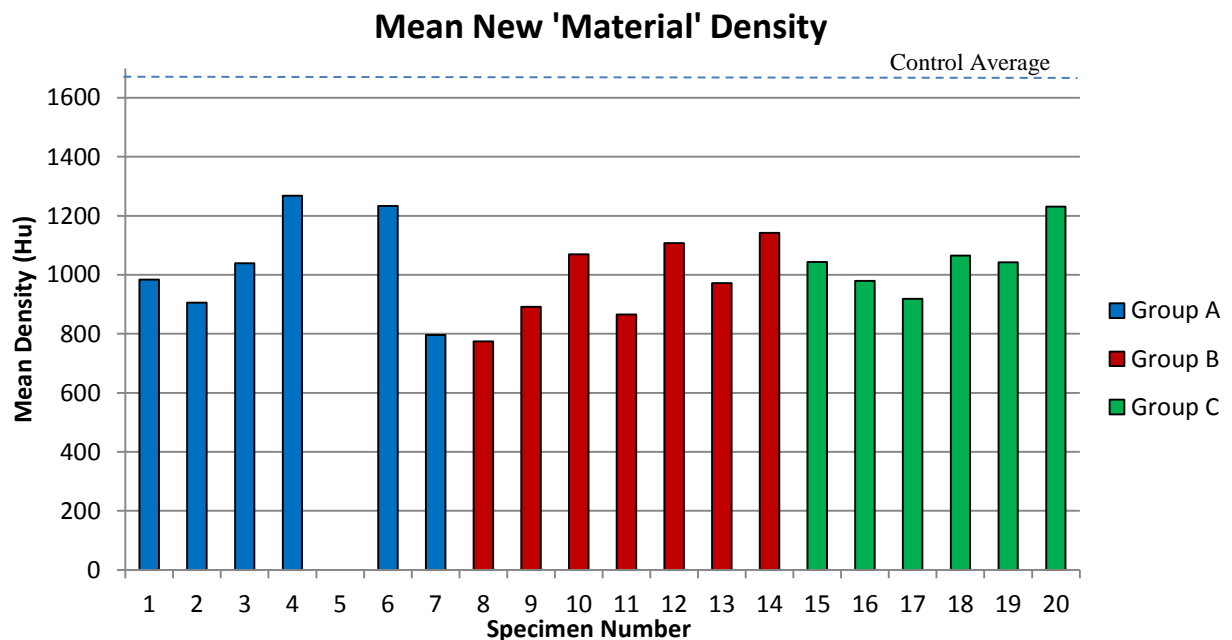


Figure 4.13. New Material mean density shown in all specimens from all groups with the average control mean density displayed with a dashed blue line.

The observed trend in figure 4.13 is all specimens have a lower mean density than the control. Group A contains the highest mean density specimen (specimen 4) with group B containing the lowest of the specimens that displayed new material formation (specimen 8). Group C had the highest mean density percentage of the control average of 64%, with group B having 60 and group A having 54%.

4.3.8. New Material Density and Volume Correlation

Similar to in the scaffold section, trends observed in the groups in terms of volume and density can indicate one groups ability to promote and sustain new material formation.

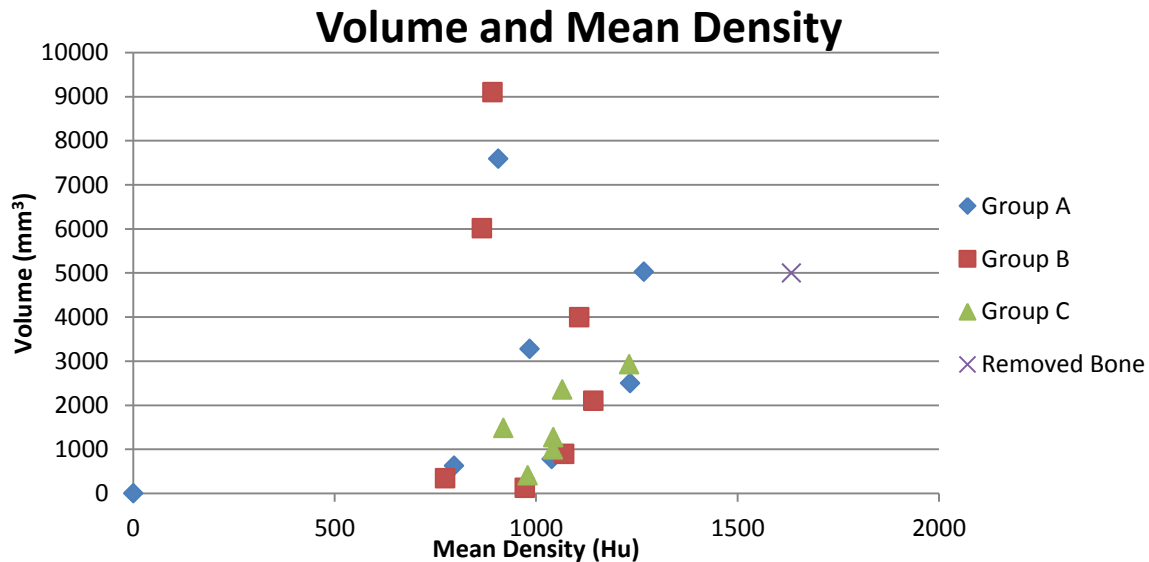


Figure 4.14. Volume and Mean density correlation in new material formations from the three specimen groups and removed bone section.

It can be said that the specimens with higher volume but lower density than the removed bone section may have early callus formation while specimens with lower volumes but increased density may have mal-union between proximal and distal tibia sections.

4.3.9. New Material Density Distribution

New material density distribution can display similarities in density regions between new material formation and existing control bone indicating if the remodelling process is more successful on one group over another.

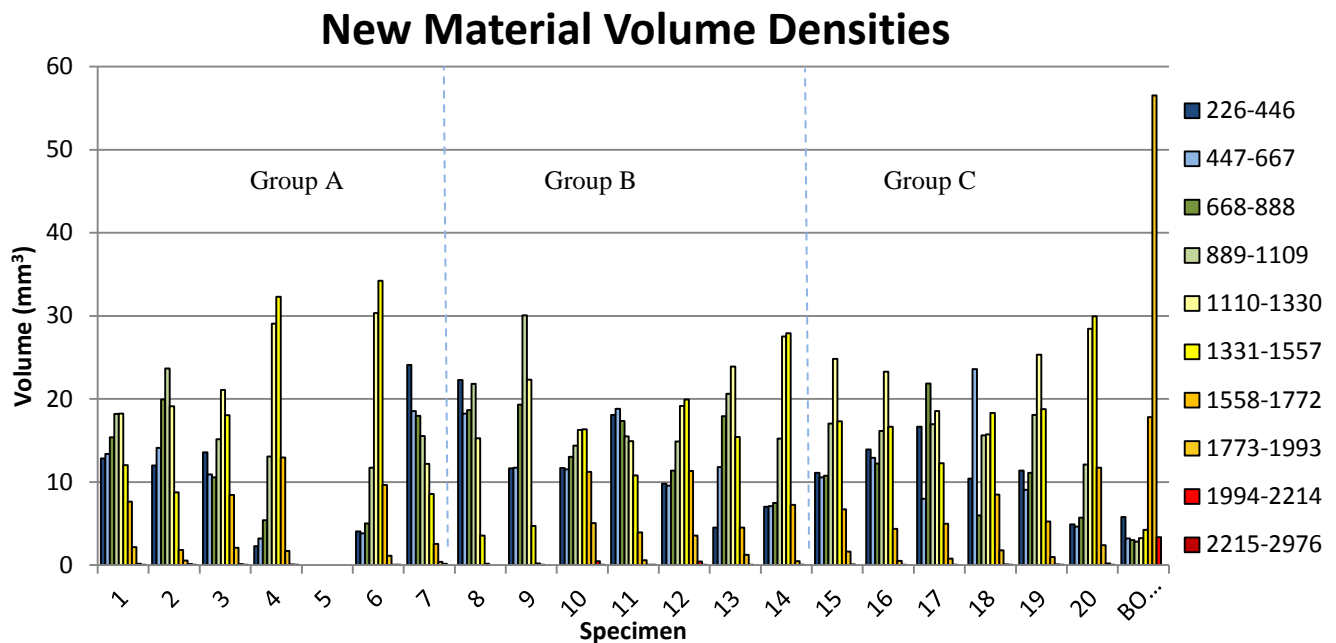


Figure 4.15. New Material Density Ranges.

Figure 4.15 shows that groups A, B and C all display a higher percentage of low-mid density volumes with less than 10% of the groups consisting of 1773-1993 HU and the control bone having almost 60% of the total volume in this region.

4.3.10. New Material Density Distribution Slices

Observing new material density distribution can give indications of the quality of the new material formations and also to identify possible signs of callus formation.

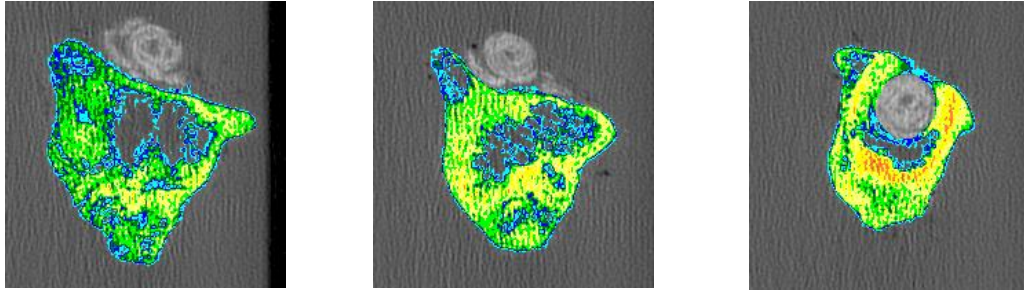


Figure 4.16.a, b, c High cross section volume with low density distribution throughout.

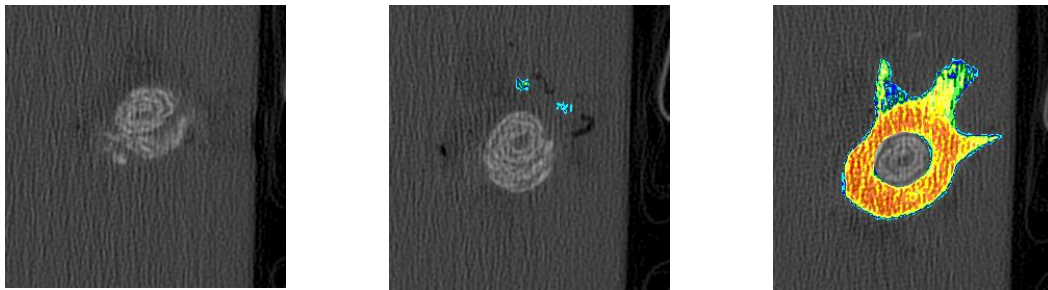


Figure 4.17.a, b, c Minimal gap closure and similar density distribution to control bone at fracture ends.

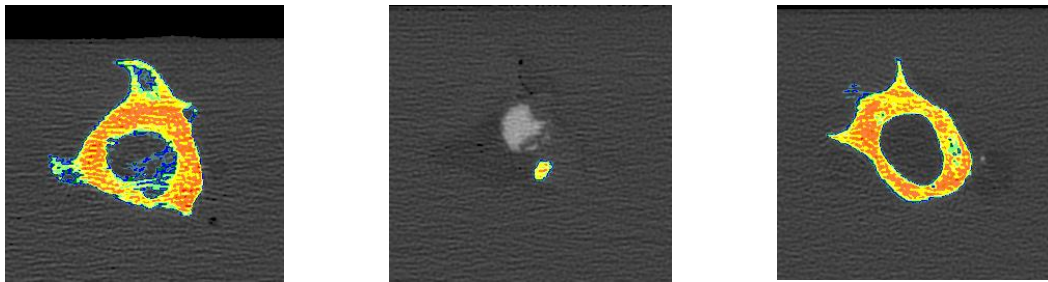


Figure 4.18.a, b, c Minimal Gap closure and similar density distribution to control bone at fracture ends.

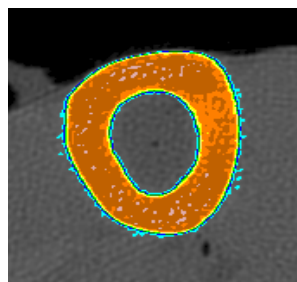


Figure 4.19. Removed Control Bone Section.

Table 4.2. Density Regions of new material.

Density Range (Hu)
226-446
447-667
668-888
889-1109
1110-1330
1331-1557
1558-1772
1773-1993
1994-2214
2215-2976

Specimens with high new material volume growth were observed to have low density distribution throughout (figures 4.17 a, b, c) while also displaying an irregular new material formation cross sectional area which is an indication of callus formation. Specimens which displayed similar density at the fracture ends to the control bone (figure 4.20) have minimal new material growth in the fracture gap (figures 4.18, 4.19) which is an indication of mal-union and the failure to heal the fracture.

4.3.11. Absolute Screw Movement

The formation of new material can be influenced by mechanical stimulation provided by the screws which hold the fracture plate to the bone. These were observed to be moving (section 3.6.4) and so the screw movement was measured to provide some correlation between new material and the mechanical stimulation to determine if the screw movement was positive or negative in stimulating the remodelling process (figure 4.20).

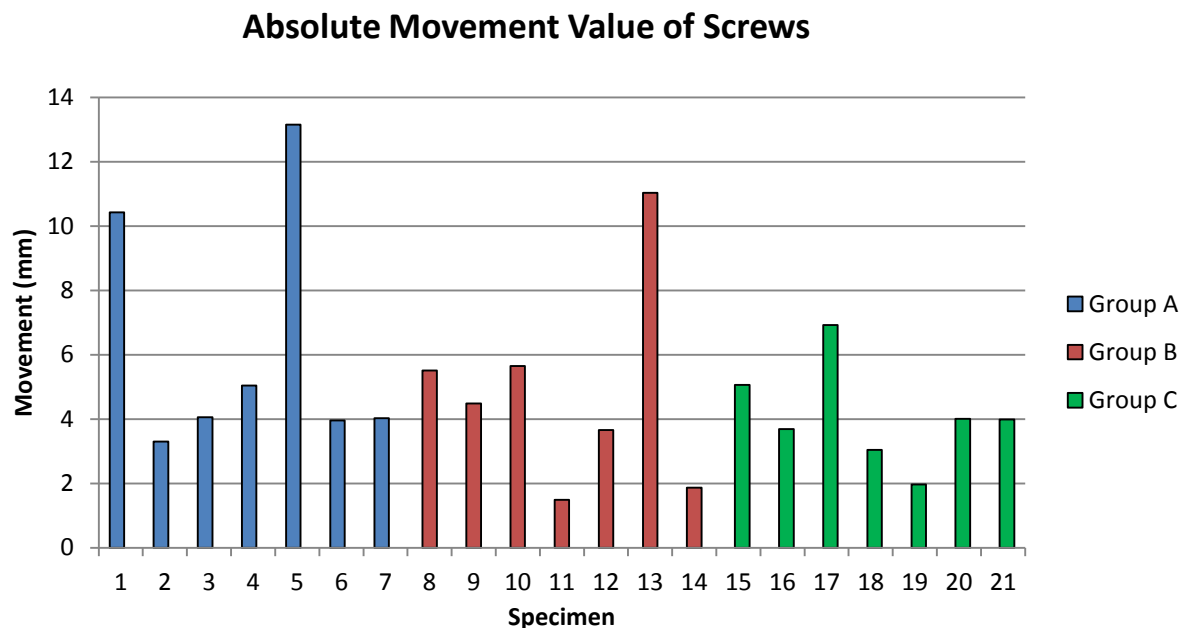


Figure 4.20. Absolute Movement of screws for the three groups.

Group A received most screw movement with an average of 6 mm, with group B averaging 5 mm and group C averaging 4 mm. There is the possibility that some groups performed better than others because the scaffold material received a critical amount of stimulation, while the other groups may have received excessive or insufficient stimulation to promote material growth. Apart from specimens 1, 5, 13 and 17, most specimens experienced a similar amount of screw movement ranging from 1.49 – 5.65 mm.

4.3.12. New Material volume, density and screw movement correlation

This section displays any correlations that could be observed between absolute screw movement with new material volume and new material density using data collected in sections 4.3.6, 4.3.7 and 4.3.11.

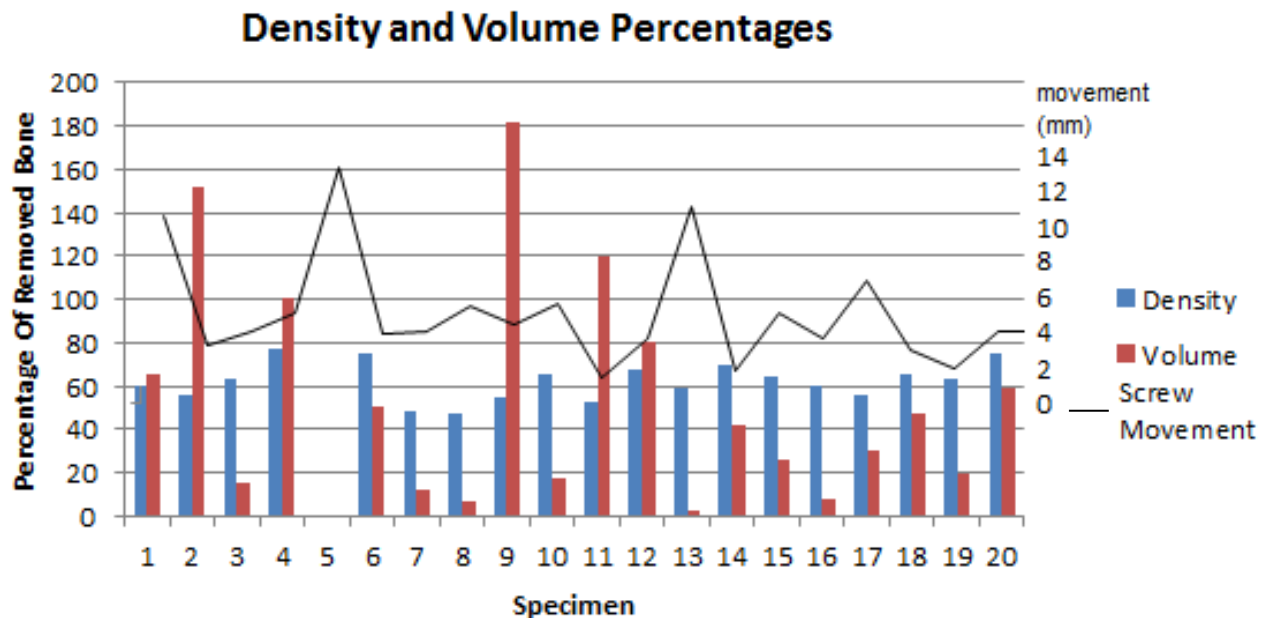


Figure 4.21. New material density, volume and absolute screw movement for each group.

The data in figure 4.21 shows that the three specimens with the largest new material formation (specimens 2, 9 and 11) all experienced small amounts of screw movement (<6 mm). Specimens 5 and 13 received the two greatest amounts of screw movement and show little or no signs of new material formation. It can also be observed that specimen 5, which experienced a fracture of the fixation plate, received the most movement (13 mm) which have caused the fracture of the plate, or be a result of the fracture. From the data it is difficult to decide what is a positive amount of dynamic movement, and what is a negative amount.

4.3.13. Proximal and Distal Density Loss

Screw reaction forces can have both positive and negative effects of the remodelling process. Density losses in the proximal and distal sections were measured to determine if the remodelling process was similar in both sections or if the remodelling process was being affected by the fixture.

Table 4.3. Density values (HU) of proximal and distal volumes showing pre and post-surgery procedures proximally and distally and also losses proximally and distally and percentage loss proximally and distally.

Specimen	pre-prox(Hu)	pre-dist(Hu)	post-prox(Hu)	post-dist(Hu)	lossProx(Hu)	lossDist(Hu)	%lossProx	%lossDist
2	1520.0	1643.0	998.8	1235.4	521.2	407.6	34	25
4	1559.3	1615.0	1398.8	1301.7	160.4	313.2	10	19
6	1507.5	1609.1	1355.3	1314.5	152.2	294.5	10	18
7	1573.7	1587.2	1012.3	1242.6	561.4	344.6	36	22
11	1533.0	1589.4	973.9	1160.8	559.1	428.6	36	27
12	1628.8	1659.3	1138.5	1224.3	490.3	435.0	30	26
13	1621.1	1647.1	1530.9	1371.3	90.2	275.9	6	17
14	1502.2	1548.9	1197.1	1180.9	305.1	368.0	20	24
16	1520.9	1620.0	1346.8	1243.8	174.1	376.3	11	23
17	1579.5	1612.1	925.8	1022.4	653.7	589.7	41	37
19	1597.5	1640.6	1415.9	1316.7	181.6	323.9	11	20
20	1565.2	1576.2	1400.1	1343.5	165.2	232.7	11	15
total -							258	272

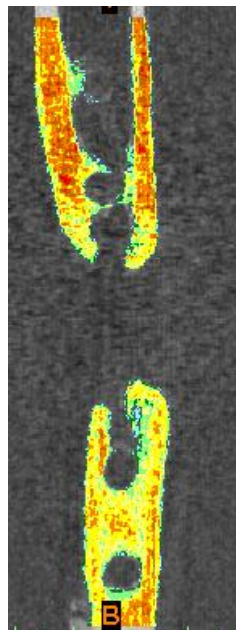


Figure 4.22. Density distribution in proximal and distal sections. Higher density materials are shown with darker colours.

It is important to notice that losses occur both proximally and distally (table 4.3) . Of the 12 specimens observed 7 of the specimens display a greater loss in the proximal side with 14%

overall greater loss in the distal sides than in the proximal side, this may be due to an increased amount of screw movement in the proximal side providing an increased level of mechanical stimulation, or too much screw movement in the distal side having a negative effect on the remodelling process (figure 4.22).

4.4. Finite Element Analysis

As shown in the previous section, density losses in the distal section are greater than in the proximal section, to identify if the screw reaction forces may be the cause of this, FEA was used to determine the screw reaction forces. Stress shielding due to the fracture fixation was also determined to display the negative effect the fixation has on the remodelling process although being a necessity to the healing process.

4.4.1. Screw reactions

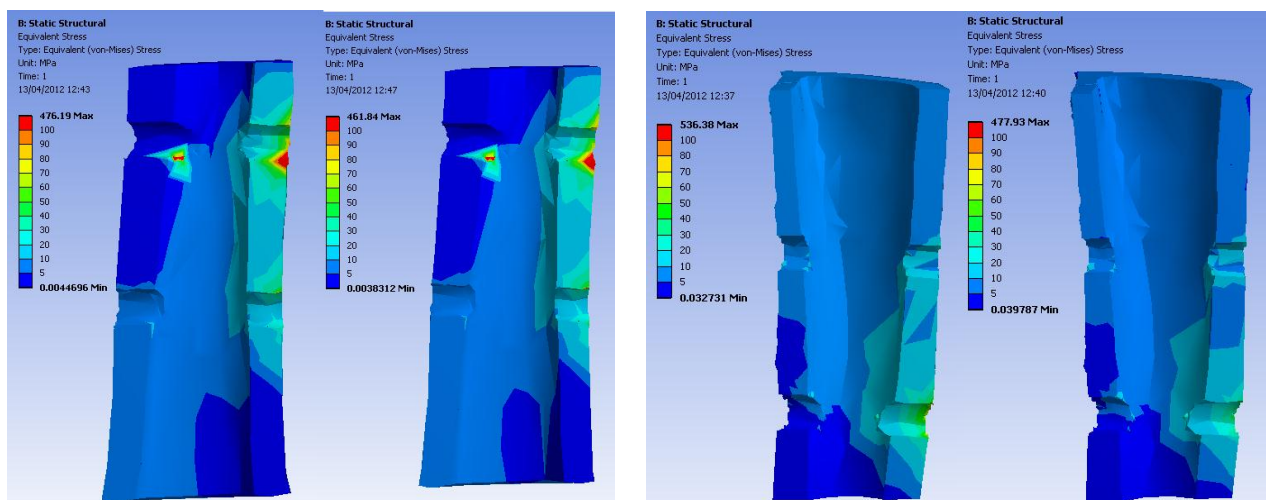


Figure 4.23.a, b Stresses on distal and proximal section of bone showing homogeneous density (left specimens) and applied CT density data (right specimens).

Figures 4.23 a and b show that the max stresses in the proximal and distal sections as a result of the screw forces are very similar. The stress distribution patterns throughout the sections are also very similar. Although the forces on the proximal side are slightly larger, there is not an obvious difference to indicate the loss in the distal side compared to the proximal side.

4.4.2. Stress Shielding

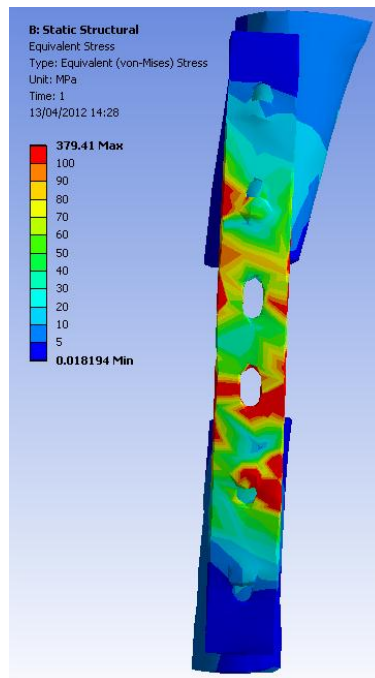


Figure 4.24. Stresses shown on fixture plate with anatomically correct and identical cross section all with homogeneous density distribution.

Varying stress concentration locations distributed throughout the plate indicate the stresses are being distributed throughout the plate. The plate displayed lower max stresses than those found in the CT applied density models which may show that density has an effect on the transition of forces throughout the bone. The plate also displays torsion as is evident from the lateral movement between the proximal and distal sections; this is probably due to the dimensions of the bone.

5. Discussion

This thesis provides analysis and displays quantitatively the effect the implant of a biomaterial scaffold has on the formation of new material in a fracture gap. Most notably it can be observed that all groups displayed to some extent new material growth. Some specimens in group A had a greater new material volume growth than some specimens in groups B and C which shows that although the scaffolds do assist in the remodelling process, in some cases the body is able to heal without external aid. In all of group B the scaffolds have increased in volume which shows new material growth inside the scaffold structure while in group C there is a large reduction in scaffold volume. This could be due to unidentifiable scaffold structure during segmentation or the biological breakdown of the scaffold during the trial. Both scaffold groups display an increase of density compared to their respective control scaffolds showing new material growth is of a higher density demonstrating the remodelling process. Only four specimens out of the 21 had a similar or greater new material volume than the removed section. This increase in volume coupled with the lower densities is also found in secondary healing callus formations showing the bone is healing in an expected way. Some of the specimens showing minimal new growth may never have fully healed if given the opportunity and simply healed into two separate sections of bone and would have required the fixture to remain in place to enable walking.

It can be seen that external stimulation effects the healing process as the specimens with the two highest values of screw movement display the lowest new material volume growth, while the specimens displaying the largest new material volume do not have the lowest values of screw movement, this is consistent with the theory that too much or not enough stimulation have negative effects on the remodelling process which is in agreement with the scientific community that static and dynamic fixations devices can have both positive and negative effects as shown in a recent test [32]. Here, 4 fixation methods (2 static and 2 dynamic) have shown inconclusive results as to which is the superior fixation method. Although all fixation methods reached 100% stiffness after 10 weeks, the dynamic fixator in type one had a greater initial stiffness growth, while the static fixator in type two had the greater initial stiffness growth, showing neither method worked better than the other in this case. The higher stress values found in the proximal section coincides with the higher density retention value although screw pull-out is primarily found in the proximal section indicating that while the dynamic properties associated with the movement of the screws can be beneficial, there are also negative sides if the movement is uncontrolled.

The present study describes techniques employed to define and quantify the formation of new material in a fracture gap undergoing a biomaterial scaffold implant. The validation of one scaffolds ability to promote quicker and more effective remodelling in comparison to a competitor would require a larger study group to provide a clear trend. All the specimens had the same living conditions and were of similar weight and age to allow for direct comparisons between results.

The study was limited by the following factors. The injured leg was not immobilized to ensure only the scaffold had an influence on the remodelling process, ideally the sheep would not apply weight on the leg avoiding external mechanical stimulation. The study groups were too small to give definitive results; larger study groups may have shown a trend indicating the more superior method to promote bone remodelling. More remodelling time may have shown increased new material growth and allowed for finite element analysis on the remodelled bone sections.

6. Conclusions

The technique employed during this trial display a clear and concise method to quantify new material growth in bone resection undergoing biomaterial scaffold implant. The results conclude that new material to some extent could be observed in all groups. Some specimens displayed the beginning of mal-union while other specimens displayed signs similar to that found in callus formation in the fracture gap. External stimulation factors played a significant role in the remodelling of the fracture gap and have shown that they can have both positive and negative effects on the formation of new material. This study displays the potential for these techniques to aid in the analysis and development of prototype and existing biomaterial scaffold technology.

References

- [1] P. Lichte, H.C. Pape, T. Pufe, P. Kobbe, H. Fischer - Scaffolds for bone healing : Concepts, materials and evidence. 2011.
- [2] <http://www.ag.ncat.edu/libbyd/SHEPLINK.HTM>.
- [3] <http://en.wikipedia.org/wiki/Bones>.
- [4]. P.C. LaStayo, K.M. Winters, M. Hardy – Fracture Healing, Bone Healing, Fracture Management and Current Concepts Related to the Hand. 2003.
- [5] L. Weiss – Cell and Tissue Biology, 6th Edition. 1990.
- [6]P.J. Nijweide, E.H. Burger, H.M. Feyen – Cells of Bone: Proliferation, Differentiation and Hormonal Regulation. 1986.
- [7] <http://www.cancer.gov/>.
- [8] H. Sievänen – Immobilization and Bone Structure in Humans. 2010.
- [9]J.H.C. Wang - Biomechanics, Model Mechano-Biology. 2006. 1–16.
- [10] H.M. Frost - Anat. Rec. 2003.
- [11]C.H. Turner- Bone. 1991.
- [12]. P.A. Hill. Bone Remodelling - British Journal of Orthodontics. Vol. 25/1998/101-107.
- [13]. D.L. Bartel, D.T. Davy, T.M. Keaveny – Orthopaedic Biomechanics, Mechanics and Design in Musculoskeletal Systems. 2006.Pearson, Prentice, Hall inc.
- [14] J. Wolff. Das Gesetz der Transformation: Transformation der Knochen. 1982.
- [15] J. Brennwald - Fracture healing in the hand, Clinical Orthopaedics. 1996.
- [16] B. McKibbin - The Biology of Fracture Healing in Long Bones. 1978.
- [17] G.G. Nemeth, M.E. Bolander, O.R. Martin - Growth Factors and their Role in Wound and Fracture Healing. 1988.
- [18] S.R. Brader, D.J. Fink, A.I. Caplan - Mesenchymal Stem Cells in Bone Development: Bone Repair and Skeletal Regeneration. 1994.
- [19] M.E. Bolander - Regulation of Fracture Repair by Growth Factors. 1992.
- [20] P.R. Blenman, D.R. Carter, G.S. Beaupre - Role of Mechanical Loading in the Progressive Ossification of a Fracture Callus.1989.
- [21] R.A. Brand - Fracture Healing. 1979.
- [22] M.C. van der Meulen, K.J. Jepsen, B. Mikic. Understanding bone strength: size isn't everything. Bone 2001;29:101-4.
- [23] J.D. Currey, K. Brear, P. Zioupos. The effects of ageing and changes in mineral content in degrading the toughness of human femora. J Biomech 1996;29:257-60.
- [24] K. S. Davison, K. Siminoski, J.D. Adachi, D. A. Hanley, D. Goltzman, A. B. Hodsmann, R. Josse, S. Kaiser, W. P. Olszynski, A. Papaioannou, Louis-George Ste-Marie, D. L. Kendler, A. Tenenhouse, J. P. Brown. Bone Strength: The whole is greater than the sum of its parts 2006.
- [25] F. Rauch, E. Schoenau - Changes in bone density during childhood and adolescence: an approach based on bone's biological organization. J Bone Miner Res 2001;16:597-604.
- [26] A.M. Parfitt. The two faces of growth: benefits and risks to bone integrity. Osteoporos Int 1994;4:382-98.

- [27] M.H. Lafage, R. Balena, M.A. Battle, M. Shea, J.G. Seedor, H. Klein, et al. Comparison of alendronate and sodium fluoride effects on cancellous and cortical bone in minipigs. A one-year study. *J Clin Invest* 1995;95:2127-33.
- [28] <http://orthoinfo.aaos.org/topic.cfm?topic=A00196>.
- [29] M. Bhandari, P. Tornetta 3rd, B. Hanson, M.F. Swiontkowski. Optimal internal fixation for femoral neck fractures: multiple screws or sliding hip screws?. *J Orthop Trauma*. Jul 2009;23(6):403-7.
- [30] R.W. Lindsey, S. Ahmed, S. Overturf, A. Tan, Z. Gugala. Accuracy of lag screw placement for the dynamic hip screw and the cephalomedullary nail. *Orthopedics*. Jul 2009;32(7):488.
- [31] R. Lakatos, M. A. Herbenick – General Principles of Internal Fixations. 2009.
- [32] R. Hente, J. Cordey , B.A. Rahn , M. Maghsud, St. von Gumpfenberg , S.M. Perren - Fracture healing of the sheep tibia treated using a unilateral external fixator. Comparison of static and dynamic fixation.
- [33] J. S. Carson, M.P.G Bostrom - Synthetic bone scaffolds and fracture repair. 2007.
- [34] J.R. Porter, T.T. Ruckh, K.C. Popat. Bone tissue engineering: A review in bone biomimetics and drug delivery strategies. *Biotechnol Prog* 2009;25:1539–60.
- [35] S.J. Peter, M.J. Miller, A.W. Yasko, M.J. Yaszemski, A.G. Mikos. Polymer concepts in tissue engineering. *J Biomed Mater Res* 1998;43:422–7.
- [36] www.gaitrite.com.
- [37] J. Hsieh – Computed Tomography : Principles, design, artifacts and recent advances.
- [38] <http://www.sprawls.org/resources/CTIMG/module.htm>
- [30] P. Gargiulo, T. Helgason, P. Ingvarsson , S. Knútsdóttir, V. Gudmundsdóttir, S. Yngvason-Morphological changes in rectus femoris muscle: advanced image processing technique and 3-dimensional visualization to monitor denervated and degenerated muscles treated with functional electrical stimulation -. 2007.
- [40] MIMICS student edition course manual.
- [41] David V. Hutton.2004. Fundamentals of Finite Element Analysis. McGraw Hill inc.
- [42] L. Peng, J. Bai , X. Zeng, Y. Zhou .2005. Comparison of isotropic and orthotropic material property assignments on femoral finite element models under two loading conditions. *Medical Engineering & Physics* 28 (2006) 227–233.
- [43] S. Kim, S. Chang, H. Jung. 2010. The finite element analysis of a fractured tibia applied by composite bone plates considering contact conditions and time-varying properties of curing tissues. *Composite Structures* 92 (2010) 2109–2118.
- [44] P. Gargiulo, T. Helgason, P. J. Reynisson, B. Helgason, H. Kern, W. Mayr, P. Ingvarsson, U. Carraro. 2011. Monitoring of Muscle and Bone Recovery in Spinal Cord Injury Patients Treated With Electrical Stimulation Using Three-Dimensional Imaging and Segmentation Techniques: Methodological Assessment. *Artificial Organs* 35(3):275–281.